Burns & Trauma, 2022, 10, tkac033
https://doi.org/10.1093/burnst/tkac033
Review

Review

Bridging wounds: tissue adhesives' essential mechanisms, synthesis and characterization, bioinspired adhesives and future perspectives

Kaige Xu, Xiaozhuo Wu, Xingying Zhang, and Malcolm Xing*

Department of Mechanical Engineering, University of Manitoba, Winnipeg, Manitoba R3T 2N2, Canada

*Correspondence. Email: Malcolm.Xing@umanitoba.ca

Received 19 November 2021; Revised 29 April 2022; Editorial decision 22 May 2022

Abstract

Bioadhesives act as a bridge in wound closure by forming an effective interface to protect against liquid and gas leakage and aid the stoppage of bleeding. To their credit, tissue adhesives have made an indelible impact on almost all wound-related surgeries. Their unique properties include minimal damage to tissues, low chance of infection, ease of use and short wound-closure time. In contrast, classic closures, like suturing and stapling, exhibit potential additional complications with long operation times and undesirable inflammatory responses. Although tremendous progress has been made in the development of tissue adhesives, they are not yet ideal. Therefore, highlighting and summarizing existing adhesive designs and synthesis, and comparing the different products will contribute to future development. This review first provides a summary of current commercial traditional tissue adhesives. Then, based on adhesion interaction mechanisms, the tissue adhesives are categorized into three main types: adhesive patches that bind molecularly with tissue, tissue-stitching adhesives based on pre-polymer or precursor solutions, and bioinspired or biomimetic tissue adhesives. Their specific adhesion mechanisms, properties and related applications are discussed. The adhesion mechanisms of commercial traditional adhesives as well as their limitations and shortcomings are also reviewed. Finally, we also discuss the future perspectives of tissue adhesives.

Highlights

- Adhesion interaction mechanisms of tissue adhesives.
- Limitations and shortcomings of commercial traditional adhesives.
- Future perspectives of multifunctional tissue adhesives.

Key words: Adhesive patch, Adhesion mechanism, Nature-inspired, Tissue adhesives, Bioadhesives

Background

Surgical reconnection of wound tissues is necessary for recovery of the tissue's structure and function. For decades, researchers have been working on developing techniques for rejoining tissues. Nowadays, surgical operations are performed daily for wound sealing in order to prevent leaks, stop bleeding and promote healing. Wound closure is the last step of a surgical operation and surgeons depend on it to gather separated tissues and control bleeding [1–4]. Conventional methods, like sutures and staples, are treated as the gold standard in wound closure, and they function well in most cases. However, these methods suffer up to

30% leakage in some special application scenarios (e.g. against high pressure in lungs and arteries) [5,6]. Due to their simplicity, sutures are one of the most common ways to close injured tissues [7]. Staples are also fast and are able to decrease the infection rate more efficiently than sutures [8]. However, despite the merits of sutures, they also cause damage to healthy tissues and result in tissue trauma and possible scarring. Besides, sutures are not ideal when minimal invasion is required; in addition, they increase the chance of bacterial infection [9,10]. Although quickly performed stapling avoids these drawbacks, it is still not appropriate for intrinsically complicated procedures, such as preventing leaks of body fluids and air in blood vessels and tissues with relatively low cohesion energy like lungs, livers, spleen and kidneys [11–13]. The difficulty of using sutures and staples while operating on areas inside the body that are not easily reachable cannot be ignored; in addition, sutures and staples do not perform satisfactorily for mending bone fractures. [14] In addition, these procedures generally require further removal steps, which is time-consuming and requires the work of a skillful surgeon.

Tissue adhesives or sealants have been made as a replacement for sutures and staples since the middle of the last century. Tissue adhesives can be defined as glues or patches that are used to bind tissues to tissues, or tissues to patches, in order to control bleeding and stop gas or liquid leaking; adhesion occurs due to intermolecular interactions at the interfaces of the two surfaces [15–17]. Adhesives provide superior convenience for wound healing, such as less traumatic closure, less pain, easier operation and no post-surgical removal, and can even release drugs and growth factors to accelerate healing [18,19]. Some are applied as commercial adhesives, e.g. fibrin glue was recommended in the 1940s [20] and cyanoacrylate adhesive was widely used in the 1980s [21].

A perfect tissue adhesive should show sufficient adhesion and cohesion of tissue bonding in even relatively humid conditions, stay stable in the physiological environment, perform rapid curing in a specific environment, and exhibit biocompatibility, biodegradability, non-toxicity and non-cytotoxicity [22–24]. Sometimes, extremely high adhesion strength is not a merit, as it may lead to undesired adherence between surgical implements and tissues, or even damage tissues; an optimal balance in adhesion strength needs to be pursued. An essential feature of adhesives is liquid repulsion, as adhesives need to maintain adhesion even under aqueous conditions since the physiological environment of human tissues is likely to be aqueous.

Based on interfacial interactions, tissue adhesives can be divided mainly into three types: (1) adhesive patches containing functional groups for molecularly binding with nucleophiles (such as amines, thiols, imidazole, etc.) of tissues through intermolecular forces; (2) pre-polymer or precursor solutions of adhesives can penetrate into porous tissues and then polymerize *in situ* to form interpenetrating bonding networks to stitch tissues together; and (3) nature-inspired adhesives can generate special adhesion such as mussel-inspired catechol functional adhesion, gecko foot pad-inspired fibrillar array-like adhesion, tree frog-inspired amphibians two-phase adhesion, octopus suction cup-inspired hollow structure-related negative-pressure adhesion etc. This review will describe and characterize the mechanisms, materials and synthesis of a range of tissue adhesives.

Review

Commercial traditional adhesives

Cyanoacrylate (CA) adhesives As a commonly used commercial adhesive, CA adhesives, which have strong and rapid adhesion behavior, were chemically synthesized and first applied as superglues in households and industries. [25] The potential of CAs for use in wound closure was discovered in the 1960s. CAs can immediately bind to the target surface at 23°C without the presence of a catalyst, heat or pressure. The liquid monomers undergo exothermic polymerization to form a strong adhesion as acrylate bonds are polarized and thus ready to attack nucleophiles of weak basic substances (such as water, body tissues and blood), because of the electron-withdrawing nitrile group [26]. When used as tissue adhesives, the liquid monomers flow and penetrate into wound interfaces, providing strong covalent bonding between CAs and functional groups in the tissues (primary amines in proteins). The adhesion strength depends on the alkyl chain's length. There are four main CA adhesives based on the alkyl chain length: methyl-CA, ethyl-CA, *n*-butyl-CA and 2-octyl-CA. Short chains provide stronger polymerized networks, whereas longer alkyl chains offer more flexible bonds, which leads to higher breaking strength [27,28]. However, the CAs show toxicity to humans, since they degrade into cyanoacetate compounds and formaldehyde that cannot be metabolized and eliminated, and these can in turn cause inflammation [29]. In addition, CAs become brittle after polymerization, which leads to poor mechanical properties and an inability to coalesce with tissues when applied on soft interfaces (skin or viscera) [30,31].

Fibrin-based adhesives Another commercialized adhesive is fibrin, which is a protein existing in human blood. The first fibrin-based adhesive was introduced in the 1940s for nerve adhesion [32]. Typically, fibrin contains three main components: fibrinogen, thrombin and factor XIII. After coming together, thrombin can cleave fibrinopeptides A and B that are contained in fibrinogen to form fibrin monomers. These monomers are self-assembled as fibrin polymer clots through H-bonds. Synchronously, the thrombin can also activate factor XIII and then catalyze the crosslinking of fibrin by producing amide bonds in the presence of calcium ions. As to wound tissue, fibrinogen can interact with thrombin as described above and form unstable fibrin clots. These clots work as hemostatic agents and sealants for wounds; in addition, the fibrin can crosslink with tissue collagen (forming amides among glutamine and lysine residues). At the wound site,

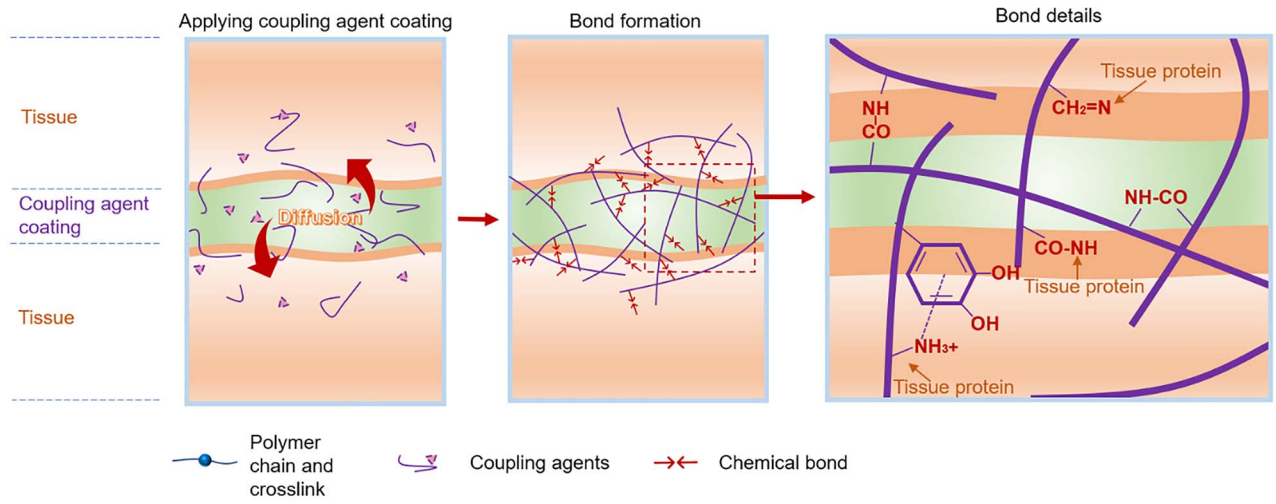

Figure 1. Adhesive molecules bind with tissue via covalent interactions of functional groups

fibrin–collagen crosslinking anchors the clots; also, platelets are activated by thrombin to provide receptors for fibrin and collagen, and then trapped in fibrin clots, which further enhance clot stabilization. Calcium ions are always needed for these reactions [33,34]. Different from CAs, fibrin-based adhesives are biocompatible and absorbable within 2 weeks [18,35]. However, they needs preparation time before use, and fibrinogen and thrombin must be stored at low temperature separately. Fibrin adhesives may transmit infectious diseases because they are made from plasma, and they may elicit an immune response and cause an allergic reaction [36,37]. In addition, fibrin adhesives have poor adhesion strength when applied to tissue, and even worse on wet surfaces [38].

Traditional gelatin adhesives Gelatin is a protein denatured from collagen via irreversibly thermal degeneration. One common gelatin-based adhesive is gelatin-resorcinol-formaldehyde (GRF), which was first introduced in the 1960s [39]; gelatin-resorcinol-formaldehyde-glutaraldehyde (GRFG) was proposed later on due to the toxicity of formaldehyde [40]. Gelatin is non-toxic and contains inherent peptide sequences. It can be crosslinked via the reaction between amines in the lysine side chains and aldehyde groups in the formaldehyde or glutaraldehyde [41,42]. When applied to wound tissue, the same reaction can be activated and the amines of tissues can be crosslinked. Usually, the GRFG adhesive components, the gelatin solution and the aldehyde solution, are stored separately. The adhesive is biodegradable via macrophage phagocytosis that starts about 60 days after use, but the degradation rate is slow. [43] During application, the toxicity of formaldehyde and glutaraldehyde cannot be ignored.

Albumin adhesives Albumin is a plasma protein in mammals. As a protein-based adhesive, similar to GRFG glue, albumin-glutaraldehyde adhesive (BioGlue®) was developed commercially in the late 1990s [44,45]. With the same reaction mechanism, the amines of lysine residues in albumin or the wound tissues can react with the aldehyde. This adhesive does not contain formaldehyde which makes it of relatively low toxicity. However, infections after use have been found because of its mammalian origin, and allergic reactions may occur [46,47].

Adhesives molecularly binding with tissue

Mechanisms The first type of mechanism relates to adhesive patches (such as adhesion polymers, hydrogels, tapes, etc.) with functional groups that can molecularly bind with diverse nucleophiles on tissue, in which the adhesives are first polymerized or gelled and then attach to the wound. The intermolecular forces between adhesive and tissues include chemically covalent interactions and physical interactions such as hydrogen bonding, ionic interactions, electrostatic interactions and van der Waals forces. For covalent interactions, usually, the adhesives provide functional groups (primary amine, aldehyde, isocyanate, carboxylic acid, phenolic hydroxy) that react with groups in the tissue (such as primary amines, carboxylic acid, thiol, hydroxy groups, etc.) (Figure 1). The physical interactions usually result in adhesion. Electrostatic interaction uses oppositely charged groups for adhesion, and hydrogen bonding, van der Waals forces and ionic interactions also can enhance interface adhesion energy. Tissue penetration may occur when patches are attached to wound tissues, but since the patches have already been polymerized or gelled, relatively few macromolecules diffuse into the tissues. Adhesive patches with different binding mechanisms and their performance are listed and reviewed in Table 1.

Adhesive patches rely on coupling reagents Some adhesive patches are modified with functional groups (amine or carboxyl). They cannot directly react with tissue nucleophiles (carboxylic acid or primary amines) spontaneously. Thus, coupling reagents like *N*-hydroxysuccinimide (NHS) and

Table 1. Adhesives that molecularly bond with tissues

Components	Adhesive design concept	Characteristics	Adhesion test on tissue/organ/substrate	Adhesion property		Ref.
				Lap shear strength (maximum, kPa)	Tensile adhesion strength (maximum, kPa)	
PAM, alginate-Ca^{2+}	Double-networks based on covalently bonding and physical interaction, in which the matrix dissipates energy under deformation	Dissipate energy, Wet adhesion	Porcine skin, cartilage, heart, artery, liver. Beating porcine heart	The highest adhesion energy is 1000 J/m^2		[48]
G-MA, gelatin, chitosan and, PAA-NHS	Wipe off interfacial water, then cause rapid crosslinking to the surface; react with amines on tissue	Wet adhesion	Lap shear and tensile adhesion tests on porcine stomach, heart, liver, skin and intestine	Maximum shear strength is 120 on porcine skin	Maximum tensile strength is 120 on porcine skin	[49]
Polydextran-aldehydes	Adhesion sponge contains aldehyde groups that can react with amines on tissues	Wet adhesion, rapid hemostasis	Adhesion test on pigskin, hemostasis on rabbit liver model	Maximum adhesion strength is 104.2 kPa		[50]
PEG-amine, dextran-aldehydes	Aldehyde-induced sealant, in which the aldehyde covalently reacts with amine groups on tissues	Aldehyde-amine	Tensile adhesion tests on rat duodenum, liver, lung, heart	N/A	724 (duodenum), 431 (liver), 72 (lung), 296 (heart)	[54]
G-MA, NB, GHA, LAP	Collagen-like hydrogel to glycosaminoglycans of human connective tissue	Wet adhesion, mobile tissues adhesion	Burst pressure tests on porcine carotid artery	The highest burst pressure that can be maintained is 300 mm Hg		[56]
Tannic acid, PAA, cellulose nanocrystals, Al^{3+}	Tannic acid-coated cellulose provided a dynamic connected bridge, the polyphenol in tannic acid showed dopamine-like catechol group adhesion on tissue	Tough, self-healing	Tensile adhesion tests on porcine skin	N/A	5.2 k (porcine skin)	[57]
Tannic acid, silk fibroin	Adhesive hydrogel relied on hydrogen bonding and hydrophobic interaction	Wet adhesion	Tensile adhesion tests on rabbit liver, heart, skin	N/A	8.5 (liver) 9 (heart) 10 (skin)	[58]
HA-epigallocatechin gallate, HA-tyramine	Epigallocatechin gallate-HA and tyramine-HA react with tyrosinase showing fast enzyme kinetics and form crosslinked adhesive hydrogel	Wet adhesion	Adhesion test on mouse dorsal skin tissues, heart, kidney. *In vivo* hepatic hemorrhage model	Maximum adhesion energy is 8 J/m^2		[59]
P(NaSS-co-DMAEA-Q)	Polyampholyte hydrogel with surface charges to neutralize tissue charges, then adhesion	Wet adhesion	Lap shear adhesion tests on porcine heart	1.6 N (porcine heart)	N/A	[64]
PNAG, hydroxyapatite	Adhesive hydrogel based on crosslinking by hydroxyapatite contains Ca^{2+} ionic bonding with OH^- and hydrogen bonding	Self-adhesive, rapid adhesion	Lap shear tests on porcine skin, myocardial tissue, pig's colon, and rat skin	105 (pigskin)	102 (pigskin) 40 (colon)	[65]
PVA with various alkyl (3, 6, and 9) methylene carbons	Hydrophobically modified alkyl groups anchored to the skin cell membranes showed strong interfacial adhesion modification	Wet adhesion	Lap shear adhesion test, and T-peel test on porcine skin	2.24 kPa for lap shear, 10.4 N/m for T-peel	N/A	[76]
PNHAM, tannic acid	Hydrogen-bonding induced coacervate adhesive hydrogel	Antibacterial, hemostatic	Lap shear adhesion test on porcine skin	38.51 (porcine skin)	N/A	[77]

(Cotinued)

Table 1. Continued

Components	Adhesive design concept	Characteristics	Adhesion test on tissue/organ/substrate	Adhesion property		Ref.
				Lap shear strength (maximum, kPa)	Tensile adhesion strength (maximum, kPa)	
PAM, alginate-Ca^{2+}	Adhesive hydrogel dissipates energy during separation, and the networks of hydrogel form strong and sparse interlinks with tissues	Water resistance	Tensile adhesion tests on porcine cartilage, skin, lung, liver and stomach	N/A	720 J/m2 (cartilage), 400 J/m2 (skin), 310 J/m2 (lung), 300 J/m2 (liver), 290 J/m2 (stomach)	[78]
Acrylic elastomer (VHB 4905, 3 M), PAM, chitosan	Bond-stitch topology adhesion	Water resistance	*In vivo* adhesion tests on rat skin	N/A	N/A	[79]
CS-aldehydes, CS-methacrylates	Aldehyde-induced bonding. Aldehydes covalently bond with amine groups of the collagen in the host tissue	Same concept inspired from wall paint	Fill cartilage defect	N/A	N/A	[80]
PSC, PEG, 2-octyl cyanoacrylate	Bone adhesive	Facilitate cell ingrowth for bone fracture healing	*In vivo* adhesion tests for mouse cranial fracture healing	N/A	N/A	[81]
PVA	PVA hydrogel with tuneable crystallinity on substrates, then dries and anneals to increase the crystallinity. Hydrogen bonds between nanocrystalline domains and solid substrates surface	Underwater adhesion	T-peeling off adhesion tests on glass, ceramic, Ti, Al, steel, PU, PDMS. Ball-on-flat sliding adhesion tests between stainless steel and chicken tibia cartilages	7500 J/m^2 (glass), 470 J/m^2 (ceramics), 225 J/m^2 (Ti), 370 J/m^2 (Al), 420 J/m^2 (PU), 150 J/m^2 (PDMS). 5000 cycles and 100 N compression force for ball-on-flat test		[82]
PAA, PDMAPAA, PNIPAM	Oppositely charged polyelectrolytes grafted with thermoresponsive PNIPAM chains	Underwater adhesion, thermo-responsive	Underwater probe-tack adhesion tests on glasses, PAA, PDMAEMA, PTFE	1.8 J/m^2 (glasses), 2.0 J/m^2 (PAA), 3.2 J/m^2 (PDMAEMA), 3.9 J/m^2 (PTFE)		[83]
Tannic acid, silk fibroin, hydroxyapatite	Adhesive for fracture fixed and accelerated bone regeneration	Wet adhesion	Tensile adhesion tests on porcine bone. *In vivo* adhesion tests on rat femur fracture model	N/A	922.83 (porcine bone)	[84]
HA-norbornenes, HA-hydrazides and HA-aldehydes	Electrospun adhesion hydrogel contains aldehyde groups, which covalently bind with amine groups on tissues	Force responsive self-adhesive	Adhesion tests on fiber hydrogels (aligned or non-aligned)	Maximum adhesion strength is 11 kPa		[85]
Polypeptides, Zn^{2+}	Metal cross-linkable proteins form stiff hydrogels with Zn^{2+}	Self-adhesive	Lap shear adhesion tests on two hydrogels (self-adhesive)	172 N/m	N/A	[86]

(Cotinued)

Table 1. Continued

Components	Adhesive design concept	Characteristics	Adhesion test on tissue/organ/substrate	Adhesion property		Ref.
				Lap shear strength (maximum, kPa)	Tensile adhesion strength (maximum, kPa)	
Ammonolysis-based tetra-PEG	Cyclized succinyl ester groups in hydrogel matrix provide quickly degradable and controllably dissolvable properties	Rapid gelation for fast adhesion	*In vivo* adhesion tests on rabbit liver	N/A	N/A	[87]
Four-arm-PEG, lysozyme	Lysozyme provides free amines to rapidly react with PEG. Lysozyme shows antibacterial and cell affinity	Injectable, antibacterial, promote healing	Adhesion test on pigskin, burst pressure test on pig abdominal aorta veins. *In vivo* adhesion tests for rabbit tracheal defects sealed and femoral artery	250 mmHg for burst pressure		[88]
Four-armed PCL-NHS	Melted PCL-NHS glue applied on a wound, then solidification to provide cohesion	Glue gun releasing	Tensile adhesion tests on rat skin	N/A	1.6 N (rat skin)	[89]
PEGSD, Fe^{3+}, UPy-HDI-gelatin	The adhesive hydrogel includes catechol-Fe^{3+} coordination crosslinked network, and quadruple hydrogen bonding crosslinked network	Injectable, self-healing	Lap shear adhesion tests on pigskin. *In vivo* adhesion tests on mouse skin	3.04 (pigskin)	N/A	[90]
Degummed silk fiber, Ca^{2+}, silk fibroin	Ca ions react with coil chains of silk by metal-chelate complexes. The metal-chelate bonding and water-capturing of Ca ions enhanced the viscoelasticity of silk. The carboxylic acids can interact with hydrophilic parts of the silk fibroin chain (like C=O, OH and $NH3^{+}$ groups)	Stretchable, reusable	Lap shear tests on pigskin. *In vivo* adhesion tests on mouse back	400 N/m (pigskin)	N/A	[91]
TEMPIC, TATATO, hydroxyapatite particles	The acidic monomers can dissolve hydroxyapatite and ionically bind to calcium ions forming precipitates into the bone surface	Thiol-ene adhesive	Lap shear tests on rat bone. *In vivo* adhesion tests on rat femur	9000 (rat bone)	N/A	[92]
Gelatin, k-carrageenan, poloxamer 407, PNIPAM-co- BA, tannic acid	TA modified substrates/tissues coating with a thermal sensitive polymer. Temperature-induced phase-change results in cohesive failing, which thus produced reversible adhesion	Reversible, thermally responsive	Tensile adhesion tests on porcine skin, porcine sclera and porcine cornea	N/A	240 J/m^2 (porcine skin), 38 J/m^2 (porcine sclera), 42 J/m^2 (porcine cornea)	[93]
Acrylated adenine, MA, AA	Copolymerization of hydrophilic and hydrophobic monomers in mixed DMSO and water solvents	Diverse solvents adhesion	Lap shear adhesion tests between gels and aluminum substrates in water, seawater, high-salt, DMSO, chloroform, ethanol, hexane, bean oil	The maximum adhesion strength is in ethanol 13.2 kPa	N/A	[94]

PNAG poly (N-acryloyl 2-glycine), *PVA* poly(vinyl alcohol), *PAA* poly(acrylic acid), *PNHAM* poly (N-hydroxyethyl acrylamide), *NHS* *N*-hydrosuccinimide, *PAM* poly(acrylamide), *NB* *N*-(2-aminoethyl)-4-(4-hydroxymethyl)-2-methoxy-5-nitrosophenoxy) butanamide, *GHA* glycosaminoglycan hyaluronic acid, *LA*: lithium phenyl-2,4,6-trimethylbenzoylphosphinate, *P(NaSS-co-DMAEA-Q)* sodium 4-vinyl-benzenesulfonate and (2-acryloyloxyethyl)-trimethylammonium chloride quaternary, *CS* chondroitin sulfate, *PSC* P_2O_5-SiO_2-CaO, PEG: poly(ethylene glycol), *HA* hyaluronic acid, *PDMAPAA* poly(dimethylaminopropyl acrylamide), *PNIPAM* poly (*N*-isopropyl acrylamide), *PCL* polycaprolactone, *TEMPIC* tris[2-(3-mercapto propionyloxy)ethyl] isocyanurate, *TATATO* 1,3,5-triallyl-1,3,5-triazine-2,4,6(1H,3H,5H)-trione, *PGS* poly(glycerol sebacate), *MA* methoxyethyl acrylate, *AA* acrylic acid, *PEGSD* poly(glycerol sebacate)-co-poly(ethylene glycol)-g-catechol, *UPy* ureido-pyrimidinone, *HDI* hexamethylene diisocyanate, *BA* butyl acrylate, *TA* tannic acid

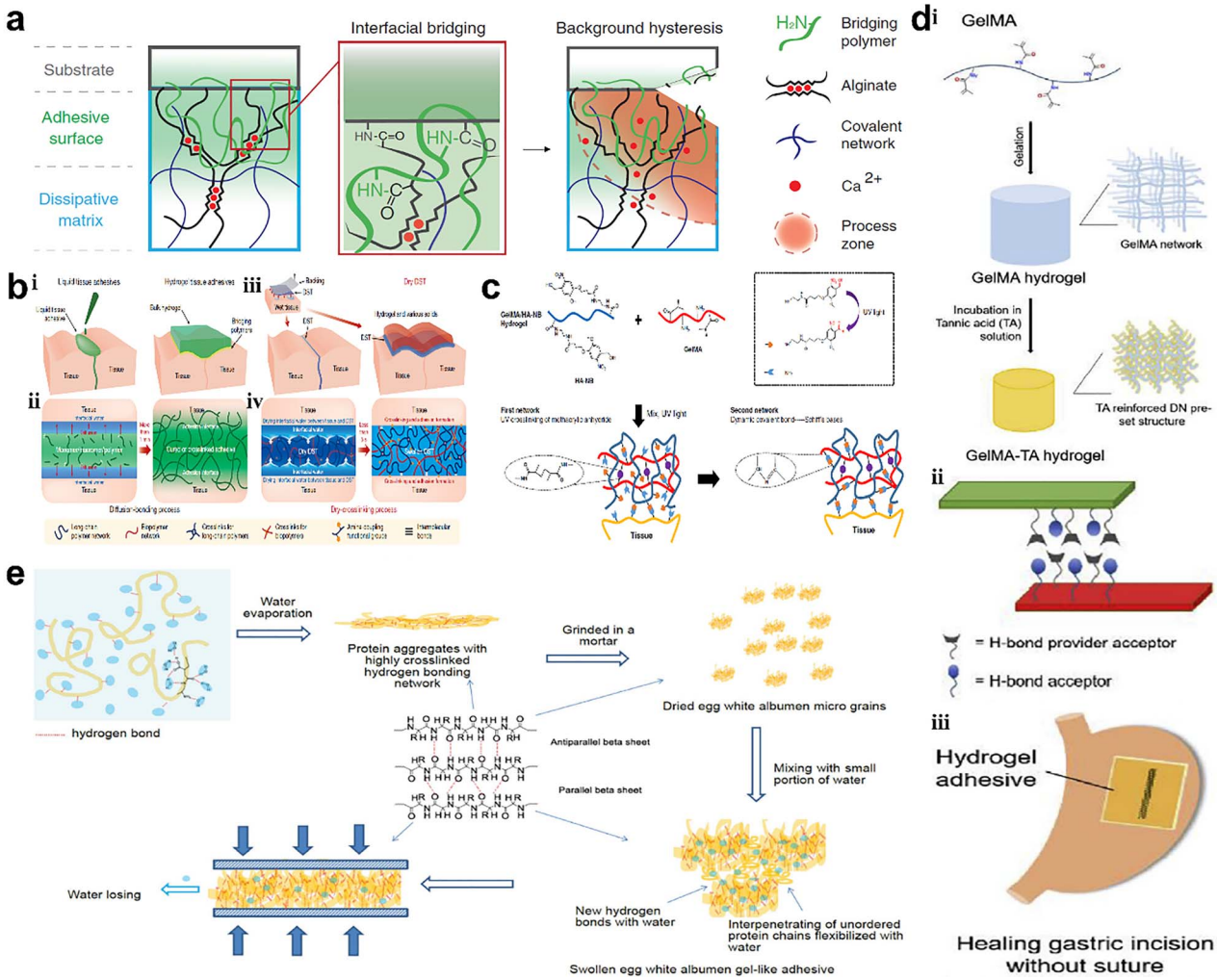

Figure 2. Adhesive patches molecularly bind to tissue. (**a**) Primary amines covalently bonding with carboxylic acids on tissues with coupling reagents (NHS and EDC). (Reprinted from ref. [48] with permission from the American Association for the Advancement of Science.) (**b**) Adhesive tapes based on carboxylic acid groups covalently bonded with primary amines on tissues to form intermolecular bonds with tissue surfaces (Reprinted from ref. [49] with permission from Springer Nature Limited.) (**c**) Photo-triggered hydrogel: the UV photo-generated aldehydes on HA-NB react with amines on G-MA; simultaneously, the generated aldehydes interact with amines on tissue. (Reprinted from ref. [56] with permission from Springer Nature Limited.) (**d**) (i) Pre-crosslinked G-MA hydrogel network strengthened by TA; (ii) G-MA-TA adhesion gel adhering to porcine skins by H-bonding; (iii) hydrogel adhesive healed gastric incision without suture. (Reprinted from ref. [61] with permission from Elsevier B.V.) (**e**) Pressure-sensitive egg white albumen adhesion on multi-substrates by intramolecular–intermolecular hydrogen bonding of peptide chains (Reprinted from ref. [66] with permission from John Wiley & Sons, Inc.) *NHS* N-hydroxysuccinimide, *EDC* (1-ethyl-3-(3-dimethylaminopropyl)carbodiimide, *UV* ultraviolet, *TA* tannic acid

(1-ethyl-3-(3-dimethylaminopropyl)carbodiimide) (EDC) are needed to facilitate the reactions.

Li *et al*. [48] developed a tough adhesive made from polymers containing positively charged amine groups (chitosan, polyallylamine, polyethyleneimine, collagen, polyacrylamide and gelatin) that could covalently bond with carboxylic acid groups on tissues with the aid of coupling reagents (NHS and EDC). The positively charged amines can also interact electrostatically with the negative groups on the tissue (carboxylic) (Figure 2a). With the help of NHS and EDC coupling, Yuk *et al*. [49] developed poly (acrylic acid) (PAA), gelatin and methacryloyl-gelatin (G-MA) based adhesives, that possess carboxylic acid groups that can covalently bond with primary amines on tissues. In addition, they can form intermolecular H-bonds and electrostatic interactions with tissues (Figure 2b).

Adhesive patches with aldehyde groups Adhesives with aldehyde groups can directly react with wound tissues without extra coupling reagents (NHS and EDC), by forming imines. This reaction is also known as the Schiff base reaction and happens in a short time [50–53]. Polysaccharides can act as adhesives in multiple ways but the most popular approach is through oxidization of a hydroxyl group into an aldehyde group via sodium periodate oxidation. The Schiff base reaction time, which is related to adhesion curing efficiency, can be tuned by the degree of oxidation. The optimum oxidation level was 50% since over-oxidation leads to overly rapid

crosslinking which does not allow sufficient time for the polysaccharide to bind to tissue, in addition to being toxic to cells.

For example, dextran was oxidized to dextran aldehyde and then formed a hydrogel with amine-modified eight-arm polyethylene glycol (PEG); meanwhile, the remaining dextran aldehyde can form imines with tissue [54]. Liu *et al*. [55] also synthesized an *in situ*-forming adhesive polysaccharide-based hydrogel, which is made from aldehyde hydroxyethyl starch and carboxymethyl chitosan. Ethylenediamine was grafted onto carboxymethyl chitosan to obtain more amino groups. Then, aldehyde hydroxyethyl starch could form a gel with chitosan and react with amines on wound tissue. In addition, Hong *et al*. [56] developed a G-MA and *N*-(2-aminoethyl)-4-(4-hydroxymethyl)-2-methoxy-5-nitrosophenoxy) butanamide (NB) linked to glycosaminoglycan hyaluronic acid (HA-NB)-based adhesive, in which aldehydes can be photo-generated under UV stimulstion of HA-NB. The aldehydes further react with G-MA and tissue, simultaneously (Figure 2c). This adhesive can polymerize and glue tissues together within seconds.

Adhesive patches with phenolic hydroxyl groups Phenolic hydroxyl groups called plant catechols that can function like mussel catechol groups are also used for adhesion. The phenolic hydroxyl groups can covalently bond with diverse nucleophiles (amines, thiol, and imidazole) from peptides and proteins on tissues. Usually, phenolic hydroxyl adhesion is achieved by introducing tannic acid (TA).

For example, Shao *et al*. [57] developed a TA surface-modified cellulose nanocrystal-based adhesive. When applied to tissue, the phenolic hydroxyl groups can work as mussel-like catechol that interacts with amines, thiol and imidazole on tissues. Beyond this, hydrogen bonding also contributes to adhesion. With the same adhesion mechanism, Dong *et al*. [58] synthesized a TA and silk fibroin-based adhesive in which the phenolic hydroxyl groups can bond with tissue through both covalent (phenolic hydroxyl-nucleophiles) and physical (hydrogen bonding) interactions. Kim *et al*. [59] fabricated a polyphenol-incorporated adhesive hydrogel for wet tissue adhesion, which is made from epigallocatechin gallate (EGCG)-modified HAs (HA-E) and tyramine-modified HAs (HA-T). The 1,2,3-trihydroxyphenyl on EGCGs showed a high affinity for tyrosinase, which made HA-E oxidize rapidly and conjugate with HA-T to generate the mixed hydrogel (HA-TE). Furthermore, the 1,2,3-trihydroxyphenyl moiety is oxidized by tyrosinase to produce activated quinone that is the same as the catechol functional groups in mussel-inspired adhesive products. In this way, oxidized 1,2,3-trihydroxyphenyl moieties can bond with multiple nucleophiles (such as amine, thiol, imidazole or other phenolic moieties) on tissue via non-enzymatic reactions [60].

However, besides phenolic hydroxyl groups, the abundant hydroxyl groups of TA can provide enhanced hydrogen bonding. [61] TA-G-MA adhesive gel was made by a two-step operation: the crosslinked G-MA hydrogel was firstly synthesized and then soaked in TA solution to form a TA-reinforced double network structure (Figure 2d). Thus, TA-G-MA gel patches could be used on porcine skin or gastric surface for wound closure. In addition, it showed good adhesion on the wet surface as hydrogen bonding enhanced the adhesion.

Adhesive patches based on physical interactions Unlike adhesive patches that mostly rely on covalent bonding, adhesives based on physical bonding show repeatable adhesion. Physical interactions usually include hydrogen bonding, Van der Waals forces, hydrophobic interactions, etc. Alternatively, the charge-balance concept provides a novel adhesion strategy. To balance the surface charge, the opposite charged adhesive and tissue can glue together [62,63].

Roy *et al*. [64] synthesized a charge-balanced polyampholyte adhesive hydrogel via ionic bonds, which was made from sodium 4-vinyl-benzenesulfonate (NaSS) and (2-acryloyloxyethyl)-trimethylammonium chloride quaternary (DMAEA-Q). As reported, this polyampholyte adhesive can adhere to either a positively or negatively charged tissue surface through mild dynamic ionic interactions. For example, positively charged PDMAPAA-Q gel could glue onto the negatively-charged liver surface, but negatively charged PNaAMPS gel could not. The advance of this adhesive was that the adhesion behavior could be repeatable since no permanent reaction occurs between tissue and the gel system; however the adhesion strength may be an issue.

In addition, another physically bonding-only concept was introduced to synthesize a strong adhesive. Cui *et al*. [65] developed a self-adhesive hydrogel via radical polymerization, which was made from *N*-acryloyl 2-glycine (ACG) and hydroxyapatite (Hap). First, poly (*N*-acryloyl 2-glycine) (PACG) was crosslinked via XL-1000 UV, then the side chains (carboxyl) formed can create both H-bonding interactions and ionic crosslinking of carboxyl-Ca^{2+} with Hap nanoparticles to create a high-strength hydrogel. When gluing on target substrates (tissues or inorganic surfaces), the carboxyl groups can offer strong hydrogen bonding; also, the introduced Ca^{2+} (Hap nanoparticles) will adsorb PACG chains and expose more chain ends outward, which allows more carboxyl groups to come into contact with the substrate surface and adhere strongly to it via more hydrogen bonding.

Advanced materials for adhesion patches that molecularly bind with tissue

Non-synthesized materials Most of the tissue adhesive patches summarized above were fabricated from synthesized materials. Even though some of the adhesives were derived from natural materials, in order to modify them with functional groups, chemicals had to be applied. These synthesis or modification processes may introduce some undesired chemicals and may cause potential toxicity. As one of the requirements for an ideal tissue adhesive is that it be non-toxic, non-chemically modified natural materials may be an option.

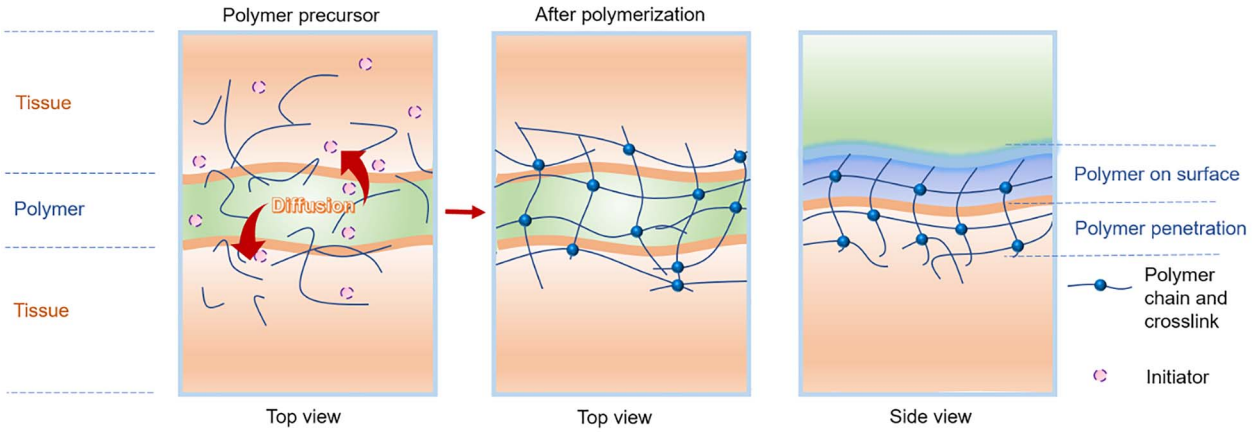

Figure 3. Tissue-stitching adhesives: pre-polymerized or precursor solutions penetrating and diffusing into tissues and forming crosslinked networks to stitch tissues together

Xu *et al*. [66] developed a fast and strong pressure-sensitive medical adhesive glue that was made from natural egg white albumen via a simple and ecologically friendly method: the fresh egg white albumen was taken and air-dried (Figure 2e). The adhesion mechanism could be explained by hydrogen bonding network formation and conformation changes of egg white albumen proteins. Egg white albumen can build strong interactions with substrates by hydrogen bonds and van der Waals forces.

Hydrophobic adhesive hydrogels (potential use as tissue adhesives) Adhesive hydrogels have proved to have strong adhesion. However, their aqueous swelling behavior may limit their application on fluid-abundant tissue wounds (vessels, livers, uterus, etc.) since hydrogels are usually formed through crosslinking of hydrophilic polymer chains and are able to hold a large volume of water [67]. Therefore, the hydrogels may need to be made hydrophobic to avoid aqueous swelling. Oliveira *et al*. [68] manufactured a hydrophobic hydrogel by coating hydrophobic microparticles on a G-MA surface. First, 1H,1H,2H,2H-perfluorodecyltriethoxysilane (PFDTS)-modified diatomaceous earth (DE) particles were made. Then, a hydrophobic hydrogel was obtained by crosslinking the PEDTS-DE microparticle-containing G-MA prepolymer under UV light. The gel exhibited liquid repelling properties and could float on the water surface. Inspired by this design concept, hydrophobic materials may be added to adhesives to solve the issue of swelling when they are used in fluid-abundant wound tissues. The adhesion mechanisms on tissue may be via hydrophobic interactions, hydrogen bonding or even electrostatic interactions [69–73]. In addition, hydrophobicity can lead platelets to aggregate, which promotes blood clotting and accelerates wound closure [74,75].

Among the adhesives listed in Table 1, a modified PVA-based adhesive was designed from the concept of hydrophobically modified alkyl groups anchored to the skin cell membranes and showed strong interfacial adhesion [76]. Hydrogen-bonding created a coacervate adhesive hydrogel that contains TA and also showed antibacterial ability [77]. Adhesive hydrogels dissipate energy during separation and exhibit strong and sparse interlinks with tissues [78]. Furthermore, an acrylic elastomer (VHB-4905, 3 M)-based adhesive was designed from the concept of bond-stitch topology [79]. Since the aldehyde group could covalently bond with amine groups, the aldehyde-modified adhesive was applied to fill a cartilage defect [80]. Apart from these well-performing adhesive patches, more adhesives with special properties were designed successfully, such as cell ingrowth-facilitating bone adhesive [81], water-proof adhesive [82–84], force responsive and self-adhesion adhesive [85,86], fast-adhesion adhesive [87], injectable adhesive [88–90], reusable adhesive [91–93] and diverse solvents-adhesion adhesive [94].

Tissue-stitching adhesives

Mechanisms Due to the porous nature of tissue, adhesives that do not rely on covalently bonding with tissue's nucleophile groups can be applied to wounds. As pre-polymerized precursors, they can penetrate and diffuse through the tissue interface to self-crosslink upon stimulation with visible light, ultraviolet light (UV), etc. (Figure 3). In this way, the wound tissues can be linked together by the formation of interpenetrating networks between tissues (Table 2). Visible and UV light are sources frequently used to initiate the crosslinking. In addition, physical interactions such as hydrogen bonding, Van der Waals forces, ionic interactions and electrostatic interactions can act as co-workers to enhance the adhesion.

Diffusion followed by light crosslinking Gelatin-based stitching adhesion can be achieved using a pre-polymer solution of G-MA combined with photo initiators followed by crosslinking [95]. Before crosslinking, the G-MA penetrates into wound tissue interfaces, and after crosslinking, the penetrated solutions form interpenetrating networks to stitch wound tissue together.

Table 2. Tissue-stitching adhesives

Components	Adhesive design concept	Characteristics	Adhesion test on tissue/organ/substrate	Adhesion property		Ref.
				Lap shear strength (maximum, kPa)	Tensile adhesion strength (maximum, kPa)	
NaSS anionic, methyl chloride quarternized DMAEA-Q cationic	Polyampholyte adhesive hydrogels based on the opposite charged balanced between hydrogels and tissues	Underwater adhesion, fast, reversible adhesion	Underwater tensile adhesion tests on porcine heart	N/A	5 (porcine heart)	[63]
PVA	PVA hydrogel with low crystallinity on substrates then dries and anneals the samples to increase the crystallinity. Hydrogen bonding between nanocrystalline domains and solid substrates surface	Underwater adhesion	T-peeling off test on glass, ceramic, Ti, Al, steel, PU, PDMS, ball-on-flat sliding adhesion test between stainless steel and chicken tibia cartilages	7500 J/m^2 on glass, 470 J/m^2 on ceramics, 225 J/m^2 on Ti, 370 J/m^2 on Al, 420 J/m^2 on PU, 150 J/m^2 on PDMS; 5000 cycles, 100 N compression force for ball-on-flat test		[82]
G-MA, Eosin Y, TEA, VC	Pre-polymer solution spray and diffuse in tissues, then crosslink under visible light	Transparent bioadhesive, visible light cross-linkable	Tensile adhesion tests on porcine skin, burst pressure test on porcine intestine sheets, *in vivo* adhesion tests for rabbit corneal defect repair	N/A	90.4 (porcine skin)	[96]
				Maximum burst pressure is 63.1 kPa		
G-MA, Irgacure 2959	Hydrogel adhesives and sealant	Inexpensive, biodegradable	Lap shear adhesion tests on porcine skin, burst pressure tests on collagen sheet, *in vivo* adhesion tests for rat lung incision sealant	262 (porcine skin)	N/A	[97]
				Maximum burst pressure is 14.9 kPa		
Human tropoelastin-methacryloyl	Pre-polymer solution sprays on wound tissues, then photo crosslinked	Tunable adhesion properties, recombinant human protein tropoelastin	Lap shear adhesion tests on porcine skin, burst pressure on rat abdominal aorta, rat lung and pig lung	75.9 (porcine skin)	N/A	[98]
				Maximum burst pressure is 99.0 kPa (rat abdominal aorta) and average burst pressure is 6.2 kPa (rat lung), and the average burst pressure is 2.92 kPa (pig lung)		
PNIPAM, alginate-Ca^{2+}, silver nanoparticle	Thermo-responsive shrinkage to generate contractile forces on the skin	Thermo-responsive, antibacterial, accelerate wound closure	Tensile adhesion tests on porcine skin	N/A	Maximum adhesion energy is 175 J/m^2 on porcine skin	[99]
Chitosan, PAM	Chitosan solution spreads and penetrates in both PAM hydrogel and tissues, then crosslinks to stitch tissues together	Wet adhesion	Tensile adhesion tests on porcine liver, heart, artery and skin	N/A	110 J/m^2 (skin), 40 J/m^2 (artery), 30 J/m^2 (heart), 20 J/m^2 (liver)	[100]
Silica ludox TM-50 nanoparticle, PDMA	Nanoparticle solution enhanced the interfacial interaction	Water resistance	Lap shear tests on calf liver	25 J/m^2 (calf liver)	N/A	[106]

(Cotinued)

Table 2. Continued

Components	Adhesive design concept	Characteristics	Adhesion test on tissue/organ/substrate	Adhesion property		Ref.
				Lap shear strength (maximum, kPa)	Tensile adhesion strength (maximum, kPa)	
MgO particles, CA–PEG-block-PPG-block-PEG-dopamine	MgO particles facilitate rapid crosslinking and work as fillers to reinforce adhesion	Wet adhesion, injectable, fast curing	Lap shear adhesion tests on wet porcine small intestine submucosa. *In vivo* wound closure on bleeding of incisions on rats	141 (wet porcine small intestine submucosa)	N/A	[107]
PEDOT: PSS, PPy, PAni adhesion on amine-functionalized glass with the PU adhesive layer	Conducting polymers adhesion on modified substrates	Wet adhesion	Lap shear adhesion tests on PEDOT: PSS, PPy and PAni with PU-coated amine-modified glass, respectively.	160 (PEDOT: PSS), 39 (PPy), 37 (PAni)	N/A	[108]
PLL, GAGs, CS, HA	PLL/GAG complexes transform to compact polyelectrolyte complexes with controlled water contents and densities, CS makes this complex solid-like, HA form highly hydrated viscous-like networks with this complex	Wet adhesion, repair soft tissue	Lap shear adhesion tests on polystyrene. *In vivo* knee skin of the rabbit	900 (polystyrene)	N/A	[109]
O-DHPLA, PAA-catechol (polyanion), DMSO (polycation)	Inspired by sandcastle worms, solvent conversion triggers polyelectrolyte to obtain wet adhesion	Underwater adhesion	Underwater tensile adhesion test on glasses	Maximum adhesion energy is 2 J/m^2		[110]
Chitosan-catechol	Catechol-plasma protein interactions, chitosan enhances the function of inflammatory cells, promotes granulation then accelerates wound healing	Fluid resistance, promote wound healing, drug delivery (anticancer drugs)	Tensile adhesion tests on mouse peritoneum, burst pressure tests on intestine	N/A	42 (mouse peritoneum)	[111]
				Maximum burst pressure is 188.3 mmHg		
P(DMS/S-alt-Man)	Non-zinc-containing commercial-based formulation is modified by P(DMS/S-alt-Man) to modulate adhesive performance	Wet adhesion, prosthodontic fixative application	Tensile adhesion tests on PMMA substrates	N/A	16.8 (PMMA substrates)	[112]
Mesoporous silica nanoparticles	Porous structure enhanced the formed nanocomposite with the body fluid in wounds (strong adhesion to tissue), and active surface endows them with fast degradation	Cause acute inflammatory response to promote healing and eliminated after tissue reformation, fast degradation	Tensile adhesion tests on rat skin	N/A	5.5 N/cm^2	[113]

(Cotinued)

Table 2. Continued

Components	Adhesive design concept	Characteristics	Adhesion test on tissue/organ/substrate	Adhesion property		Ref.
				Lap shear strength (maximum, kPa)	Tensile adhesion strength (maximum, kPa)	
Acid-treated titanium film	Acid-treated titanium film showed roughened surfaces, which increase the anchor capacity of titanium to tissues	Fast adhesion for soft tissue (roughened surfaces caused protein adsorption, cell adhesion, cell differentiation)	Lap shear adhesion tests on mouse dermal tissue	64 (mouse dermal)	N/A	[114]
HAM-GC, HMHPA	Hydroxyethyl acrylamide showed outstanding super-low fouling ability, glycerol and water formed two-phases to produce a dynamically stable system. Glycerol introduced extreme temperature resistance	Antifreeze, extended air stability, anisotropic transformation	T-peeling test on solid substrates (plastic, HDPE, PTFE, rubbers, ceramics, silica glasses, glasses, carnelian, wood, stainless steel, gold, silver, aluminum, copper)	Maximum strength is 180 N/m on glasses		[115]
PAA, PAM, Fe^{3+} ions	Solution contains Fe^{3+} ions that spread and penetrate in PAA and PAM hydrogel to form coordination complexes with carboxyl groups; these complexes dissociate as Fe^{3+} is reduced to Fe^{2+} under UV exposure	Strong adhesion between two hydrogels, but adhesion is photo-detachable	T-Peeling off tests	Adhesion energy decreased after UV applied because of the photo-detachment		[116]
G-MA, Bio-IL-choline	Cardiopatch adheres to myocardium because of ionic interactions between Bio-IL and tissues. Patch pre-soaked in Irgacure solution, crosslink under UV	Conductive adhesive cardiopatch	Tensile adhesion test on cardiac tissues, burst pressure test on rat heart. *In vivo* adhesion tests on murine heart	N/A	25 (cardiac tissue)	[117]
PEGDMA	PEGDMA with nano-/micro-structural arrays on the film surface. PEGDMA can absorb large amounts of water and swell as water-responsive, then the shape-reconfigurable (nano/micro arrays on the surface) can be controlled.	Wet responsive, switchable and controllable adhesion, nano−/micro-arrays on film	Pull-off forces measurements on glass	Maximum burst pressure is 32 kPa The highest strength is 191 kPa on a dry surface, but 0.3 kPa when water applied (wet responsive)		[118]
PNaAMPS, PAM	Inks made from the precursors of the hydrogel and elastomer. During curing, covalent bonds form to interlink two polymer networks in an integrated structure	Printable, topological entanglement	T-peeling adhesion tests on glasses	Maximum adhesion energy is 1300 J/m^2		[119]

PDMA poly(dimethylacrylamide), *PEG* polyethylene glycol, *CA* citric acid, *PPG* poly(propylene glycol, *HAM* hydroxyethyl acrylamide, *GC* glycerol, *HMHPA* (2-hydroxy-2-methyl-1-[4-(2-hydroxyethoxy)phenyl] 1-acetone), *PVA* poly(vinyl alcohol), *PEDOT* poly(3,4-ethylenedioxythiophene), *PSS* poly(styrene sulfonate), *PPy*: polypyrrole, *PAni* polyaniline, *PU* polyurethane, *PAA* poly(acrylic acid), *PAM* poly(acrylamide), *NaSS* sodium p-styrenesulfonate, *DMAEA-Q* N, N-dimethylamino ethylacrylate, *PNIPAM* poly (*N*-isopropyl acrylamide), *PLL* poly-L-lysine, *GAGs* glycosaminoglycans, *CS* chondroitin sulfate, *HA* hyaluronic acid, *TEA* triethanolamine, *VC N*-vinylcaprolactam, *O-DHPLY* oxidized 3,4-dihydroxy-L-phenylalanine, *DMSO* dimethyl sulfoxide, *Bio-IL* bio-ionic, *PEGDMA* poly(ethylene glycol) dimethacrylate, *P(DMS/S-alt-Man)* poly(3,4-dimethyoxystyrene/styrene-alt-maleic anhydride), *PNaAMPS* poly(2-acrylamido-2-methyl-1-propanesulfonic sodium)

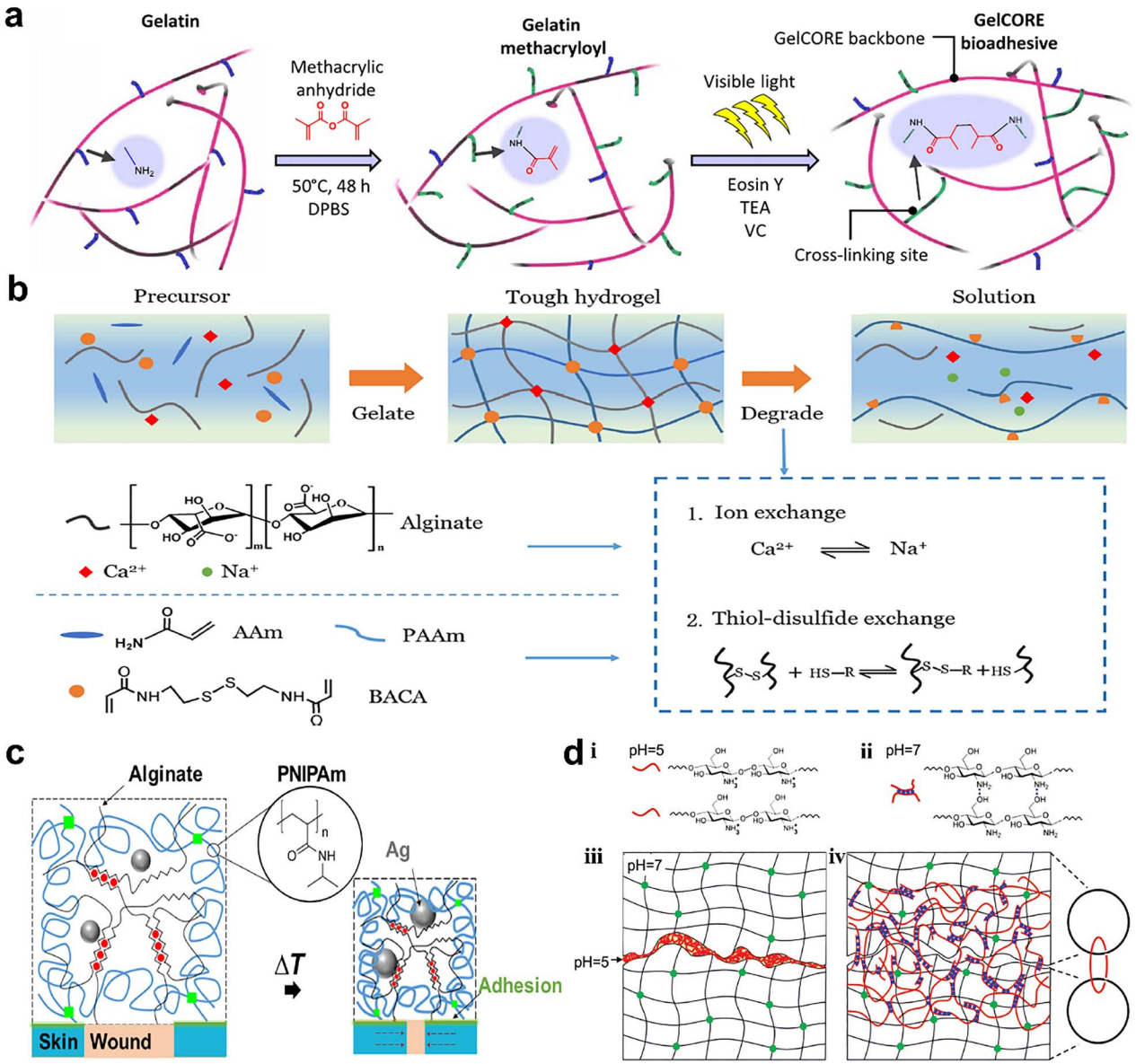

Figure 4. Pre-polymerized or precursor solution-dependent tissue-stitching adhesives. (**a**) G-MA adhesive hydrogel for corneal repair: pregel solution penetrated into the cornea for visible light-crosslinking in the presence of photo initiators. (Reprinted from ref. [96] with permission from the American Association for the Advancement of Science.) (**b**) Polyacrylamide-alginate-Ca^{2+} adhesive hydrogel glued the tissue together via chitosan-EDC-NHS spraying to form amide interlinks and physical bonding by virtue of positively charged amines and negatively charged carboxylic acid. (Reprinted from ref. [78] with permission from the American Chemical Society.) (**c**) Chitosan and coupling agents (NHS and EDC) solution penetrate into tissues and PNIPAM–alginate hydrogel to form amide bonds. (Reprinted from ref. [99] with permission from the American Association for the Advancement of Science.) (**d**) Chitosan (pH < 6.5) penetrated into two PAM hydrogels, then formed new networks via NH_2-OH hydrogen bonding as the pH increased (pH > 6.5), which became entangled with existing gel networks. (Reprinted from ref. [100] with permission from John Wiley & Sons, Inc.)

For example, Sani *et al*. [96] developed G-MA for corneal injury repair, in which the G-MA was pre-blended with a photo initiator (eEosin Y), and triethanolamine (TEA) and *N*-vinylcaprolactam (VC) as co-initiator and co-monomer, respectively (Figure 4a). After the pre-polymer penetrated into the cornea, it was crosslinked via visible light to close the wound. The UV initiator Irgacure 2959 is used most commonly. Assmann *et al*. [97] sprayed Irgacure 2959 with G-MA on tissues under UV for strong adhesion. Likewise, gelatin can offer extra adhesion to wound tissue because it has several regions that can adsorb onto cells and extracellular matrix, thereby enhancing adhesion. In order to improve adhesive elasticity, methacryloyl-modified human protein tropoelastin (Metro) was used. Annabi *et al*. [98] sprayed Metro and Irgacure 2959 pre-polymerized solution onto tissue interfaces using UV exposure for tissue binding. In addition, Metro gel can also physically entangle within tissue collagen fibers causing physical interlocking at the interfaces. Meanwhile,

positively charged tropoelastin can electrostatically interact with negatively charged glycosaminoglycans, which also improves adhesion.

Diffusion followed by EDC and NHS crosslinking As tissue-stitching adhesives, coupling reagents are also able to trigger covalent reactions between the adhesive and tissues. Usually, the coupling reagents, such as EDC and NHS, are first sprayed onto adhesives and tissues before attaching them. Thus, not only can the penetrated adhesive molecules be 'anchored' with tissues via interpenetrating network formation, but the covalent bonding can also further firmly fasten the interface adhesion.

Yang *et al*. [78] researched an adhesive containing alginate-Ca^{2+} and polyacrylamide. They sprayed chitosan containing coupling reagents (EDC and NHS) onto hydrogel and tissue, which formed amide interlinks through amines and carboxylic acid groups. In addition, the positively charged amines and the negatively charged carboxyl can physically interact together to enhance the adhesion (Figure 4b).

Furthermore, Blacklow *et al*. [99] developed a thermo-responsive adhesive that is made from poly(*N*-isopropyl acrylamide) (PNIPAM) and alginate, and achieved adhesion with the help of amines from chitosan and coupling agents (EDC/NHS) (Figure 4c). As a thermo-responsive polymer, PNIPAM repels water and shrinks when the temperature is >32°C. When placed on the skin, PNIPAM–alginate adhesive dressings can shrink to produce contractile forces, and these forces transfer to the wound edges to close the wound. In order to transfer contractile forces efficiently, PNIPAM–alginate adhesive must strongly glue on the skin. Thus, chitosan, EDC and NHS were sprayed onto tissue and PNIPAM–alginate. After penetration, tissue and adhesive can adhere together.

Diffusion caused topological entanglement Strong adhesion can be achieve by topological entanglements, without the requirement for functional groups. The pre-polymer diffuses into two interfaces (e.g. hydrogels) that have pre-existing polymer networks. After polymerization, a new network is formed to entangle the primary networks. Unlike other tissue-stitching adhesives, no initiators or coupling reagents are required. Although some adhesives rely on specific functional groups that can offer relatively strong wet adhesion, they may require complicated fabrication and inconvenient application processes. Therefore, adhesives based on topological entanglement can address these issues.

Yang *et al*. [100] placed chitosan, poly(4-aminostyrene) (PAS), alginate and cellulose onto the interfaces, respectively (Figure 4d). After diffusion of these polymer chains, pH was a trigger to make the polymer chains form new networks that became topologically entangled with the existing networks of the interfaces. Chitosan solution (pH < 6.5 for dissolution) was sprayed onto polyacrylamide (PAM) hydrogel, then another piece of PAM was placed on top for compression. The two gels can strongly adhere together since the penetrating chitosan chains (pH < 6.5) form new networks via NH_2-OH hydrogen bonding when the pH at the hydrogel interface is increased to pH 7, which become entangled with the existing PAM networks. They then applied this mechanism to various porcine tissues (liver, heart, artery and skin *in vitro*). Topological entanglement may offer an alternative method for wet adhesion since chemical reactions are not required.

Considerations for improved adhesion of advanced materials Swelling is one issue that must be considered in designing tissue adhesives. As adhesives are applied in fluid-abundant environments, water uptake will lead to a weakening at the adhesive interface. Besides, undesired swelling may squeeze surrounding tissues in confined areas [101–103]. Thus, non-swelling or negative-swelling adhesives would be promising.

Du *et al*. [104] designed a non-swelling hydrogel adhesive via the free radical polymerization of poly(ethylene glycol) diacrylate (PEGDA), Pluronic F127 diacrylate (F127DA) and modified sodium alginate (MAlg, synthesized via an amidation reaction with 2-aminoethyl methacrylate hydrochloride). The hydrogel was then coated with TA. The non-swelling property was mainly because strong hydrogen bonding between TA and poly (propylene oxide) (PPO) produces a hydrophobic effect within a 3D vinyl crosslinked network. The TA's multiple catechol groups formed robust H-bonding with dense networks of PEGDA, F127DA and MAlg, which constrained water intake. Furthermore, Barrett *et al*. [105] have manufactured negative-swelling polymer hydrogel adhesives, i.e. amphiphilic block copolymers of PPO–poly (ethylene oxide) (PPO–PEO) with catechol terminals. The catechols provide tissue adhesion, and the thermosensitive PPO–PEO blocks change from hydrophilic to hydrophobic with changes in physiological temperature, which results in gel contraction.

More tissue-stitching adhesives with highlighted characteristics are summarized in Table 2. Since almost all adhesives are used in wet conditions, water-resistance should be the first consideration for adhesive design. Due to their special tissue penetration and diffusion mechanism, tissue-stitching adhesives exhibit better water-resistance properties than other adhesives [106–112]. Furthermore, tissue-stitching adhesives with other properties performed very well, e.g. healing-promotion [113], fast-adhesion [114], antifreeze [115], photo-detachable [116], conductive [117], wet-responsive [118] and 3D-printable [119].

Bioinspired adhesives

As one of the most popular tissue adhesive approaches, bioinspired, naturally occurring adhesives include mussel protein-inspired adhesives (Figure 5a), fibrillar array-like gecko foot pad-inspired adhesive, two-phase adhesion inspired from amphibious tree frogs, adhesives inspired from Octopus suction cups (hollow structures generate negative pressure) (Figure 5b) and tree roots interpenetrating into the soil (Figure 5c), etc.

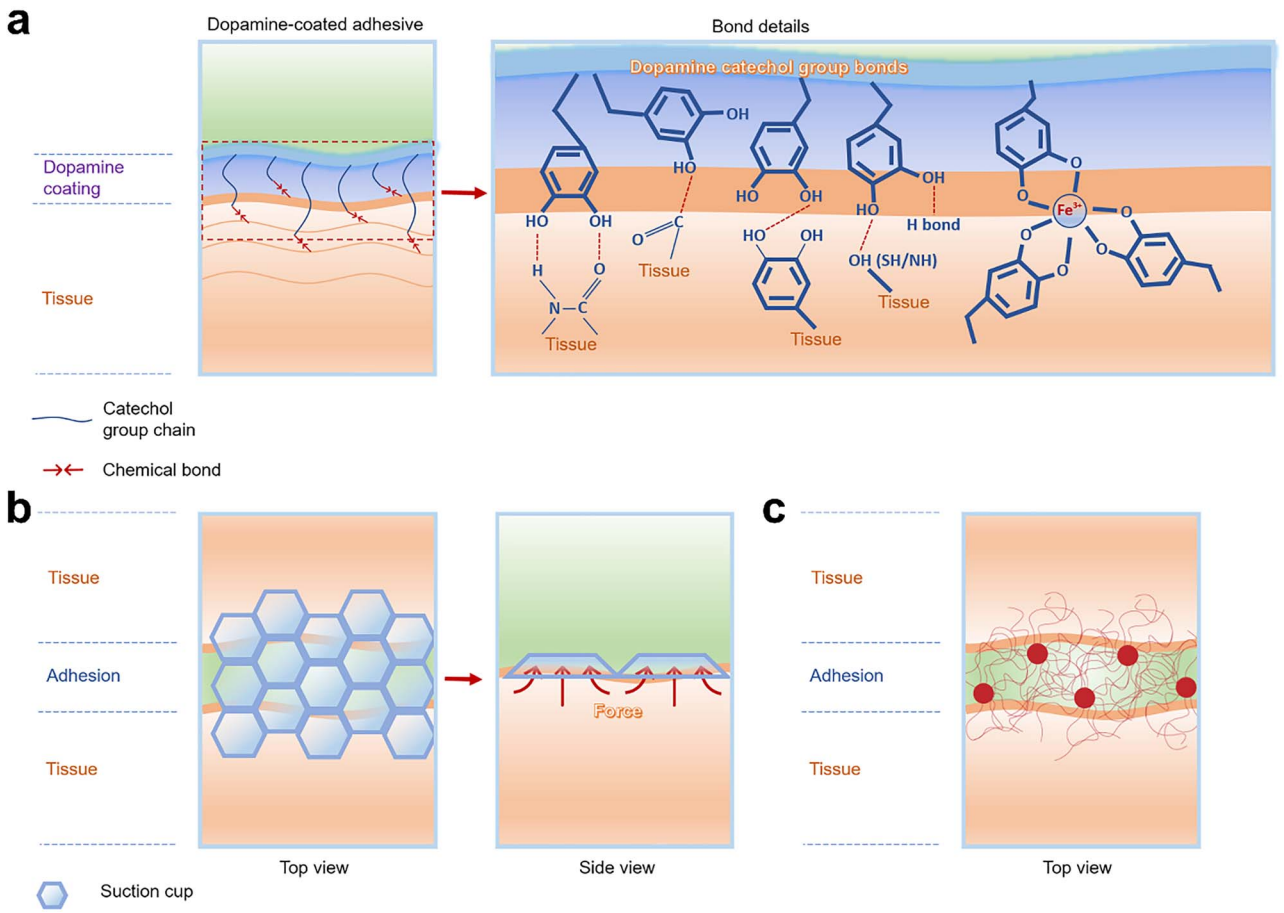

Figure 5. Adhesion mechanisms of bioinspired adhesives. (**a**) Mussel-inspired adhesives adhere to tissues through multiple interactions. (**b**) Octopus suction cups generate negative pressure for tissue attachment. (**c**) Adhesives are bioinspired from growing tree roots interpenetrating soil

Mussel-inspired adhesives Among bioinspired adhesives, one main category is the bioadhesive generated by mussels. In nature, mussels can robustly stick to the surfaces of natural structures in aqueous conditions (rock surfaces in the ocean) and can be functionalized under alkaline conditions, which mainly relies on L-3,4-dihydroxyphenylalanine (DOPA) being oxidized to form its quinone products, and adhere to target surfaces via a variety of interactions (such as chemical bonding by catechol to nucleophile groups on tissue, π–π interactions, π–cation interactions, hydrogen bonding and even metal complexation etc. (Figure 5a) [120–122]. Due to these unique advantages, dopamine has been widely used in many areas apart from for tissue adhesives [123–126]. In tissue adhesives application, mussels are usually used for wet or underwater adhesion (Table 3).

For example, inspired by the mussel, Han *et al.* [127] researched a conductive adhesion hydrogel made from polydopamine-decorated carbon nanotubes, glycerol, acrylamide (AM) and acrylic acid (AA), in which the polydopamine can interact with PAM–PAA networks via multiple interactions among catechol and carboxylic/amino groups (Figure 6a). Also, the reactive catechol on polydopamine can bind with high affinity to diverse nucleophiles (amines, thiol and imidazole) on tissue peptides and proteins.

Liao *et al.* [128] synthesized a conductive and adhesive gel that contains single-wall carbon nanotubes (SWCNTs), polyvinyl alcohol (PVA) and dopamine. Pre-oxidized and polymerized dopamine was mixed with PVA and FSWCNTs solution, in which supramolecular crosslinking was generated among FSWCNTs, PVA and polydopamine in the presence of borate by hydrogen bonds, π–π stacks and dynamic interactions between the hydroxyl groups of PVA and tetrafunctional borate ions. In addition, the oxidized catechols can covalently react with amine, imidazole and thiol residues that are contained in tissues, thus making them adhere to tissue. Much research is devoted to mussel-inspired adhesives because of their great biocompatibility and good adhesion performance even underwater.

In addition, Salzlechner *et al.* [129] developed a DOPA-modified hyaluronic acid-methacryloyl adhesive, in which DOPA can be passively oxidized in tissue environments and then the oxidized catechol chemically bonds with amine, thiol and carboxyl groups in tissues. Ruprai *et al.* [130] also developed an L-DOPA-modified porous chitosan adhesive (chitosan and L-DOPA were mixed to form a solution which was then freeze-dried to make a porous film); thus, oxidized catechol groups in L-DOPA covalently bond with amine, imidazole and thiol residues present in

Table 3. Mussel-inspired adhesives

Components	Adhesive design concept	Characteristics	Adhesion test on tissue/organ/substrate	Adhesion property		Ref.
				Lap shear strength (maximum, kPa)	Tensile adhesion strength (maximum, kPa)	
Chitosan-catechol	Mussel-inspired adhesion through catechol-conjugated chitosan	Fluid-resistant adhesion, anticancer drug delivery	Tensile adhesion tests on mouse peritoneum. Burst pressure tests on intestine	N/A	42 (mouse peritoneum) The highest burst pressure that can be maintained is 210.2 mmHg	[111]
PDA, glycerol, CNT	Glycerol provides temperature tolerance, CNT is for conduction, PDA provides mussel-like adhesion	Long-lasting moisture and extreme temperature tolerance, conductive adhesion	Tensile adhesion tests on porcine skin. *In vivo* adhesion tests on rat skin	N/A	57 (porcine skin)	[127]
DOPA, PVA, SWCNTs	Crosslinks among DOPA, PVA and SWCNTs in the presence of borates rely on H-bonds, π–π stacks and interactions between -OH of PVA and borate ions, which also provide self-healing ability.	Self-healing, self-adhesive, conductive	Tensile adhesion tests on glasses, rubber and porcine skin	N/A	9.2 (glasses), 8.3 (rubber), 5.2 (porcine skin)	[128]
Methacrylate-HA-DOPA	Mussel-inspired adhesion, gel crosslinks quickly under standard surgical light	Water-resistance adhesion	Tensile adhesion tests on mouse hind limb muscle, porcine articular cartilage	N/A	140 μN/8 mm dimeter disk hole	[129]
L-DOPA, chitosan	L-DOPA enhanced porous chitosan adhesion films. Green light enables photochemical bonding to the tissue (green light promotes crosslinking of catechol)	Wet adhesion, less water swelling	Bonding strength tests on sheep small intestine serosa	The maximum bonding strength is 25 kPa		[130]
DOPA-gelatin, DOPA-PPy, oxidized HA, hydrazide HA	Fe^{3+} induces ionic coordination between DOPA-gelatin and DOPA-PPy. Oxidized HA and hydrazide HA formed gel via Schiff base reaction	Conductive, injectable, water-resistance adhesion	Lap shear adhesion tests on porcine myocardium tissue, porcine skin	10 (myocardium), 17 (skin)	N/A	[134]
PDA, clay, PAM	PDA-inserted clay nanosheets involving free catechol formed adhesive hydrogel with acrylamide. The PAM gel contains enough free catechol groups for mussel-inspired adhesion	Super-elastic, repeatable adhesion	Tensile adhesion tests on glasses, titanium, polyethylene and porcine skin	N/A	120 (glasses), 80.8 (titanium), 80.7 (polyethylene), 28.5 (porcine skin)	[135]
PETEA, PEGda, DOPA	Hyperbranched polymer involving hydrophobic backbone and hydrophilic side-branches. Mussel-inspired adhesion and coacervates generated by self-aggregating of hydrophobic chains, which repels H_2O to enhance mussel adhesion	Underwater adhesion	Tensile adhesion tests on ceramic, Fe, PMMA, PET, PTFE, PE, glasses, wood. *In vivo* adhesion tests on rat femoral artery and liver	N/A	345 (ceramic), 390 (Fe), 320 (PMMA), 250 (PET), 127 (PTFE), 251 (PE), 205 (glasses) 211 (wood)	[136]
Thiourea-catechol functionalized gelatin	Inspired by catechol-rich Mfps and thiol-rich Mfp-6 marine mussel, thiourea-catechol-modified gelatin crosslinked quickly.	Injectable, near-native tissue mechanical properties, wet adhesion	T-peeling adhesion tests on pericardium surface. Burst pressure tests on pericardium tissue	Maximum adhesion energy is 27.09 J/m^2. Maximum burst pressure is 127.31 mmHg		[141]

(Cotinued)

Table 3. Continued

Components	Adhesive design concept	Characteristics	Adhesion test on tissue/organ/substrate	Adhesion property		Ref.
				Lap shear strength (maximum, kPa)	Tensile adhesion strength (maximum, kPa)	
Glycine, lysine, cysteine, phenylalanine, tyrosine, DOPA	DOPA modified peptides, cation–π interactions produce self-assembly and cohesion	Underwater adhesion	N/A	N/A	N/A	[142]
DMA, BA, AA	Copolymerization of DMA with pressure-sensitive adhesive monomers: butyl acrylate and AA	Pressure-sensitive, wet adhesion	T-peeling adhesion tests on polyethylene, stainless steel (dry and wet)	70 N/25 mm (dry steel), 50 N/25 mm (wet steel), 35 N/25 mm (dry polyethylene), 30 N/25 mm (wet polyethylene)		[143]
DOPA-thiol	Thiol can control the propensity of DOPA oxidation	Underwater adhesion	Lap shear adhesion tests on the bovine tooth	4500 (bovine tooth)	N/A	[144]
Suckering-12, DOPA	Cross β-sheet networks are the suckerins in the sucker ring teeth of squids. Recombinant suckerin-12 showed adhesion. DOPA is incorporated in suckerin-12	Underwater adhesion	Tensile adhesion tests on SiO_2	N/A	Maximum adhesion strength is 35.25 mN/m	[145]
PAni-co-(PDA-g-PLA)	Electro-spun nanofibers-based scaffold	Conductive scaffold, promote cells proliferation and adhesion	*In vivo* adhesion tests on mouse osteoblast	N/A	N/A	[146]
ε-poly-L-lysine-catechol, chitosan-catechol, HA-catechol, Fe^{3+}	Mussel-inspired adhesion, Fe^{3+} induced ionic coordination	Environment-dependent adhesion	Lap shear adhesion tests on collagen casing	160 (collagen casing)	N/A	[147]
Catecholic primer layer-coated PMA resin	Inspired from mussel adherence on the mineral surface through H-bonds, metal coordination, electrostatic and ionic interactions, the molecule catechol coating layer enhances the adhesion ability of PAM resin polymer	Various mineral surfaces adhesion	Lap shear adhesion tests on PMA, mica, glasses, tooth enamel	Maximum adhesion strength is 200 kPa on mica surface	N/A	[148]
PDA, CS, PAM	Due to plentiful reactive catechol on PDA, PDA-CS formation via self-assembling, then incorporated into a PAM hydrogel system. PDA shows mussel-inspired adhesion and great cell adsorption	Growth factor-free for cartilage regeneration	Tensile adhesion tests on porcine skin. *In vivo* rabbit cartilage defects repair	N/A	30 (porcine skin)	[149]
G-MA, DOPA, Ti, cationic antimicrobial peptide, SiNPs	DOPA-modified G-MA hydrogel coats on Ti implants, peptides for antimicrobials, SiNPs for osteoconduction	Prevention of infections, enhanced osteogenesis	Lap shear adhesion tests on titanium, glasses	Maximum adhesion strength is 60 kPa	N/A	[150]
Benzoxazine-catechol	Catechol functional groups modify thermoset benzoxazine monomers, catechol provide mussel-like adhesion	Bioinspired, thermal curing, high strength	Lap shear adhesion tests on aluminum	14 000 (aluminum)	N/A	[151]

(Cotinued)

Table 3. Continued

Components	Adhesive design concept	Characteristics	Adhesion test on tissue/organ/substrate	Adhesion property		Ref.
				Lap shear strength (maximum, kPa)	Tensile adhesion strength (maximum, kPa)	
Mussel adhesive protein (produced in an *Escherichia coli* expression system), silk fibroin, HA	Inspired from endoparasites that swell their proboscis to anchor to hosts' intestine, develop hydrogel formed microneedle patch coated with swellable mussel adhesion protein	Mussel protein modified microneedle protein patch, swelling mediated physical entanglement	Tensile adhesion tests on porcine skin under semi-dry and wet conditions. Burst pressure tests on intestinal tissue	N/A	150 (semi-dry porcine skin), 130 (wet porcine skin)	[152]
				Maximum burst pressure is 139.7 mmHg		
DOPA, gelatin, Fe^{3+}	Fe^{3+} forms hexavalent Fe complexes, and crosslink strands to form a metallo-adhesive with tissue proteins	Microcatheters deliverable	Lap shear adhesion tests on porcine skin. *In vivo* mice uterine injury repair	4 N/cm^2 (porcine skin)	N/A	[153]
Chitosan-MA-catechol, chitosan-MA, Fe^{3+}	Functionalized chitosan-based hydrogel formed through crosslinking of C=C and catechol-Fe^{3+} chelating interaction	Injectable, double network	Lap shear adhesion tests on porcine skin. *In vivo* mouse cutaneous defect repair and mouse liver hemorrhaging repair	17 (porcine skin)	N/A	[154]

DOPA 3,4-Dihydroxyphenylalanine, *PETEA* pentaerythritol tetraacrylate, *PEGda* poly(ethylene glycol) diacrylate, *PDA* polydopamine, *PAM* poly(acrylamide), *PPy* polypyrrole, *PAni-co-(PDA-g-PLA)* polyaniline-co-(polydopamine-grafted-poly(D,L-lactide), *HA* hyaluronic acid, *PMA* polymethacrylate, *CNT* carbon nanotube, *PVA* poly(vinyl alcohol), *SWCNTs* single-wall carbon nanotubes, *CS* chondroitin sulfate, *SiNPs* silica nanoparticles, *MA* methacryloyl, *DMA* dopamine methacrylamide, *BA* butyl acrylate, *AA* acrylic acid

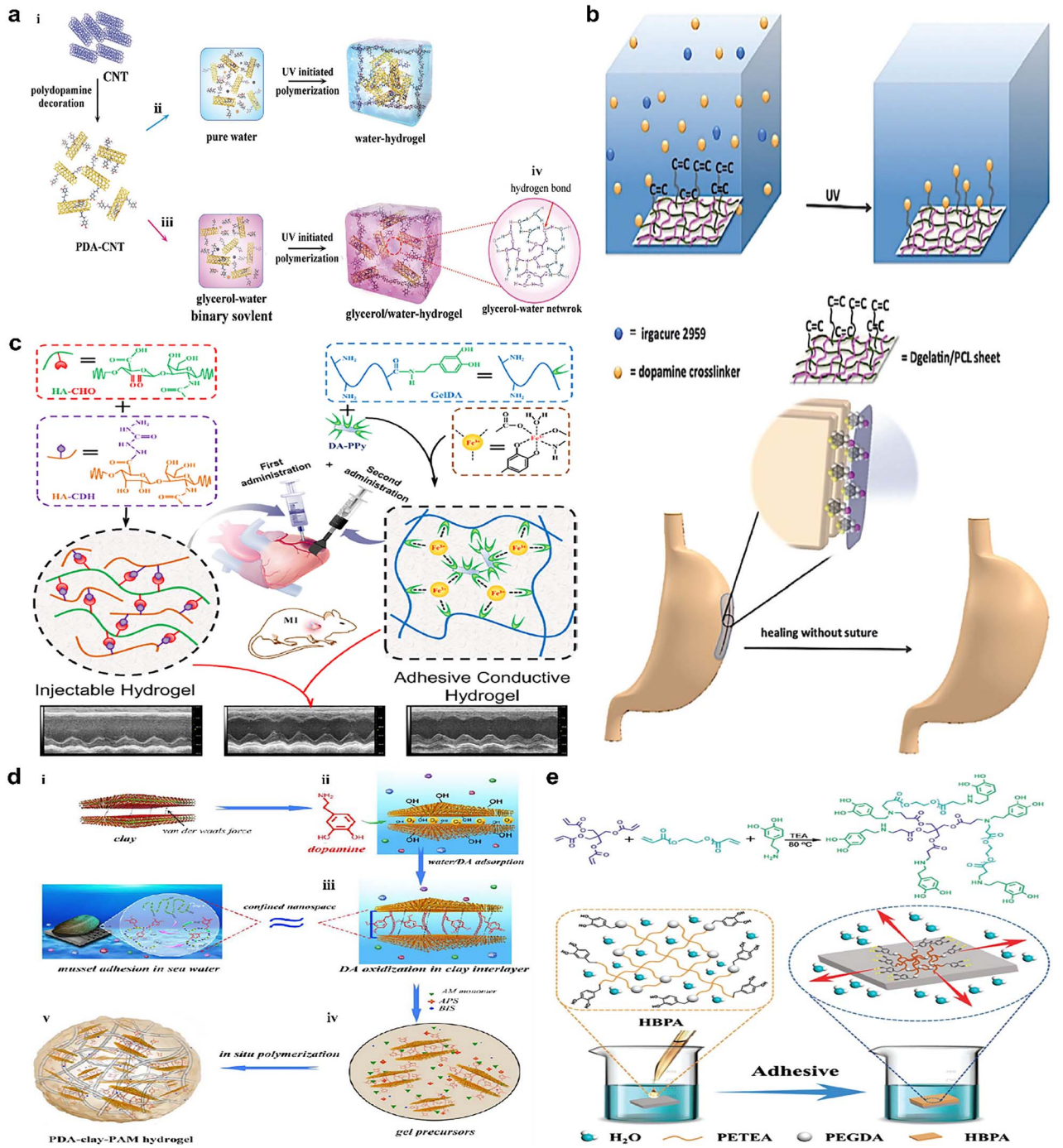

Figure 6. Mussel-inspired tissue adhesives. (**a**) Mussel-inspired conductive adhesion hydrogel: PDA–PAM–PAA networks are formed via multiple interactions among catechol and carboxylic/amino, and the reactive catechol binds with high affinity to diverse nucleophiles on tissue. (Reprinted from ref. [127] with permission from John Wiley & Sons, Inc.) (**b**) Dopamine-MBA was used as a crosslinker to conjugate with a G-MA and PCL sheet combined with I2959 under UV; the catechol groups on dopamine showed mussel-inspired adhesion to tissue. (Reprinted from ref. [131] with permission from the Royal Society of Chemistry) (**c**) Adhesive conductive hydrogel patch: Fe^{3+} induced ionic coordination of gelatin-dopamine and dopamine-Ppy networks, and the gelatin-dopamine-Ppy adhesive hydrogel patch could adhere to tissue via catechol groups. (Reprinted from ref. [134] with permission from the American Chemical Society) (**d**) Mussel-inspired adhesive hydrogel: seawater-like ions in nanoclay result in *in situ* oxidation of dopamine to form an adhesive gel with acrylamide under the action of an initiator and crosslinker; catechol groups provide tissue adhesion ability. (Reprinted from ref. [135] with permission from the American Chemical Society) (**e**) Hyperbranched polymer adhesive: hydrophilic adhesive catechol side branches and hydrophobic backbone show strong underwater adhesion due to water triggering hydrophobic chain aggregation to generate coacervates that quickly repel water, leading to the revealing of catechol groups and robust adherence to surfaces. (Reprinted from ref. [136] with permission from John Wiley & Sons, Inc)

tissue proteins, thus adhering to tissue. Jiang *et al*. [131] developed a mussel-inspired adhesion nanofibrous sheet for stomach incision healing. This adhesion sheet was made from dopamine-*N*,*N*′methylenebisacrylamide (MBA) as a crosslinker to crosslink the G-MA and PCL sheet that was synthesized via an electrically-spun technique under UV with photoinitiator I2959 (Figure 6b). The crosslinker was produced via Michael reaction of dopamine and MBA and then the G-MA/PCL nanofibrous sheet was assembled by electrospinning out the mixture solution. The MBA did not affect the catechol groups on dopamine-MBA which still worked as adhesion groups to bond with tissue. Furthermore, with the same design concept, a dopamine-MBA crosslinker was applied to gather polypyrrole (Ppy) nanoparticles, G-MA and PEGDA into a cryogel that worked as a cardiac pad for myocardial infarction treatment [132]. A mussel-inspired adhesive hydrogel made from polydopamine, nanoclay and polyacrylamide has been manufactured [133]. Instead of using oxidants that may cause inflammation ($FeCl_3$, $NaOI_4$, O_2, etc.) as curing agents to oxidize dopamine (Figure 6c) [134], nanoclay was applied, which can provide seawater-like ions to provide alkaline conditions for dopamine polymerization (Figure 6d) [135]. In addition, the clay's layered construction promoted the insertion of dopamine into the limited clay interstices, which resulted in polydopamine-inserted clay nanosheets that involved enough free catechols but was not overoxidized. Acrylamide was introduced and formed a durable adhesive hydrogel under the action of an initiator and crosslinker. Catechol groups in the polydopamine provide all the tissue adhesion ability.

For the purpose of boosting underwater or wet adhesion strength, mussel-inspired adhesive combined with a hydrophobic backbone is one of the best design strategies since catechol groups in mussel can provide wet adhesion as well as hydrophobic chains that can offer water-repelling behavior. Cui *et al*. [136] designed a hyperbranched polymer adhesive that contained hydrophilic adhesive catechol side branches and a hydrophobic backbone that can show strong underwater adhesion (Figure 6e). This adhesive, which was made from pentaerythritol tetraacrylate (PETEA), poly (ethylene glycol) diacrylate and dopamine, was prepared via Michael reaction of multi-vinyl monocase with dopamine (providing amines). When applied on a water or fluid-abundant target surface area, the water triggers the aggregation of the hydrophobic chains to generate coacervates that quickly repel water on the target surface, leading to the revealing of catechol groups and robust adherence to surfaces.

The latest research on mussel adhesion proved that, apart from catechol-rich mussel foot proteins (Mfps), thiol-rich Mfp-6 works as a significant contributor to mussels' extraordinary adhesion and rapid gelation properties [137–139]. Even though there is only 3 mol% catechol in Mfp-6, the cysteine residues can quickly crosslink with catechol-rich proteins (Mfp-3 and Mfp-5) [140]. Inspired by this function, Wei *et al*. [141] synthesized an injectable adhesive hydrogel made from thiourea-catechol-modified gelatin (G-TU-Cat), in which thiourea mimicked thiol-rich Mfp-6. As a relatively mild crosslinking condition, peroxidase from horseradish and hydrogen peroxide was used to enzymatically crosslink G-TU-Cat rapidly. When applied to tissue wounds, catechol groups in hydrogel play the adhesion role to glue the tissue together.

More wet-resistant mussel-inspired adhesives [142–145] with some other characteristics are included in Table 3. For example, mussel-inspired adhesives with conductivity may promote cell proliferation and adhesion [134,146]. Also, environment-dependent adhesives that could adhere to various mineral surfaces have been designed [147,148]. Due to the great biocompatibility of PDA, a growth-factor-free adhesive was made for cartilage regeneration [149]. With the addition of a cationic antimicrobial peptide, one DOPA-based adhesive exhibited infection prevention [150]. In addition, mussel-inspired adhesives were also designed with thermal curing ability [151] and swelling-mediated performance [152] and others that could be delivered by microcatheter [153] and were injectable [154].

Other bioinspired or biomimetic adhesives After millions of years of evolution, Nature provides alternative concepts for reliable adhesion to sophisticated surfaces. Bioinspired or biomimetic adhesives have merits that synthetic adhesives cannot match. Such merits offer rapidly reversible adhesion that has allowed geckos to walk on walls and ceilings and octopuses to stroll freely on rocks in the harsh ocean environment. The clingfish also exhibits tough adhesion in extreme and rugged ocean environments since the suction disc on the clingfish has hexagonal shapes divided by connection grooves, which can increase the water drainage rate and prevent water trapping (Table 4). As a result of water drainage, the suction disc can form a cavity chamber and generate negative pressure with the target surface, thus adsorbing on the adherend.

Rao *et al*. [63] developed an adhesive patch with a surface pattern modified with hexagonal facets separated by interconnecting grooves made from a polyampholyte hydrogel of negatively charged sodium *p*-styrenesulfonate and positively charged methyl chloride quarternized *N*,*N*-dimethylamino ethylacrylate (Figure 7a). The adhesion mechanism is via the hexagonal facets attached to the substrate that form bridges between the dynamic electrostatic bonds of the hydrogel and the substrate. This surface pattern design can accelerate water drainage and prevent water becoming trapped inside, thus giving it the potential for underwater adhesion. Similarly and serendipitously, octopus suction cups also present a hollow structure, which can generate negative pressure for anchoring purposes (Figure 5b). In the ocean, the octopus shows controllable adhesion to slippery and rough surfaces; their suckers also offer multiple capacities for movement, hunting food and recognizing tactilely [155–157]. Artificial adhesion suckers have been developed inspired by this periodic adhesion performance and has been used for wearable electronics (Figure 7b. [158–162].

Table 4. Bioinspired and biomimetic adhesives

Components	Adhesive design concept	Characteristics	Adhesion test on tissue/organ/substrate	Adhesion property		Ref.
				Lap shear strength (maximum, kPa)	Tensile adhesion strength (maximum, kPa)	
Silica ludox TM-50 nanoparticle, PDMA	Nanoparticles sticking on gels, which play as nodes in connecting polymer chains, also dissipate energy under stress	Water resistance, rapid adhesion	Lap shear adhesion tests on calf liver	Maximum adhesion energy on calf liver is 25 J/m^2	N/A	[106]
s-PUA, PET	Inspired by the dome-like protuberances and mimicked the octopus suckers' geometry, pressure differentials between the inner and outer environment	Reversible wet/dry adhesion	Tensile adhesion tests on silicon wafer substrate under dry, moist, underwater and oil conditions	N/A	25 (dry), 38 (moist), 41 (underwater), 180 (under oil)	[162]
PDMS	PDMS substrate modified with nanosucker arrays inspired from octopus' suckers	Wet adhesion	Tensile adhesion tests on glass sheets in a dry and wet environment, adhesion area is 1 cm^2	N/A	3 N (dry), 2.8 N (wet)	[164]
PDMS	Adhesion patch made with hexagonal architectures and various geometric parameters	Wet adhesion	Peeling off adhesion tests on Si wafer. Tensile adhesion tests on pigskin under dry and moist conditions	N/A	Maximum adhesion energy is 2.8 J/m^2 (dry) and 2.3 J/m^2 (wet) Peeling energy is 16 J/m^2	[165]
Anodic aluminum oxide, PDMS	Nanopile interlocking, inspired from tree roots	Tunable stretchability, and used as strain sensors	Tensile adhesion tests on the rigid rod with epoxy resin	N/A	26 000	[166]
PDMS and PVDF	Two-phases adhesive: solid–liquid, mechanical dispersion of solid spheres and liquid	Repeatable stick-on different materials, no curing time	Lap shear adhesion tests on copper	11 000	N/A	[167]
PDMS	Bioinspired fibrillar adhesives, mushroom-like fibril array	Liquid repellent	Hemispherical smooth glass probe glued to the PDMS (mushroom-like fibril array) film under dry, water, ethylene glycol, and MeOH conditions	35 mN (dry), 37 mN (water), 28 mN (ethylene glycol), 7 mN (MeOH)		[168]
PDMS	Skin adhesion films with elastomeric microfibers modified with mushroom-shaped tips	Wet adhesion	Attached to human skin with a 1 cm^2 circular area	Maximum adhesion strength is 18 kPa		[169]
Balanus albicostatus (cp 19 k) protein	Nanofibers, inspired from barnacles	Underwater adhesion	Tensile adhesion tests on mica	The maximum adhesion force is 1.6 N		[170]
Hexagonal boron nitride, rhodium (h-BN/Rh [111])	Mimicking gecko moves on a ceiling, adhesion of liquid glue on solid via static friction	Switchable wetting and adhesion		N/A	N/A	[171]
PVS	Biomimetic adhesive patch, mushroom-shaped microstructure, pillar-shaped	Microstructure surface, biomimetic	Pull-off adhesion tests by glass sphere on microstructure surface	The maximum pull-off force is 30 mN		[172]
PDMS	Bioinspired from gecko-foot, micropillar-patterned PDMS	Adhesion on the rough surface	Pull off adhesion tests on rough glass	3 kPa		[173]

PDMS polydimethylsiloxane, *s-PUA* polyurethane-acrlate, *PET* polyethylene terephthalate, *PVDF* polyvinylidene fluoride, *PDMA* poly(dimethylacrylamide), *PVS* polyvinyl siloxane

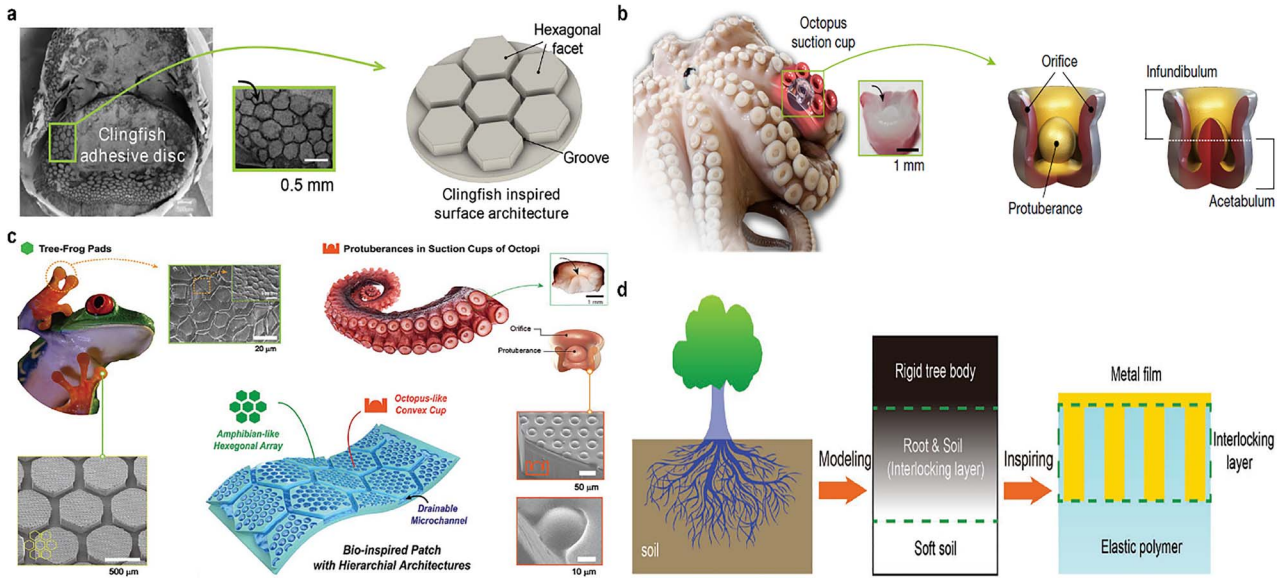

Figure 7. Bioinspired or biomimetic adhesives. (**a**) Adhesion hydrogel with water-proof adhesion ability inspired from the features of clingfish adhesion discs: hexagonal facets separated by grooves. (Reprinted from ref. [63] with permission from John Wiley & Sons, Inc.) (**b**) Adhesion patch inspired from the suction cups of an octopus: negative pressure generated by the inner hollow structure. (Reprinted from ref. [162] with permission from Springer Nature Limited.) (**c**) Bioinspired wet adhesion patch using hierarchical hexagonal structures: hexagonal structures (pads of tree frog) and protuberances with a hollow structure (suction cup of octopus vulgaris tentacle). (Reprinted from ref. [165] with permission from John Wiley & Sons, Inc.) (**d**) Adhesion patch made by nanopile interlocking inspired from the stretching of fractal roots into soft soil (Reprinted from ref. [166] with permission from John Wiley & Sons, Inc.)

Nano-suckers based on protuberant nano-balls have been produced using a solvent settlement method. UV-sensitive resin-coated polystyrene nano-spheres were soaked in high-polar solvents (like acetonitrile, nitromethane, propylene carbonate, etc.). The solvents caused the external surface of the inner nano-spheres swell but did not etch any polymers, which then formed a negative-pressure between the cavity nano-suckers and the substrates [163]. Despite their good adhesion strength, the harmful solvent may limit their application on tissues.

As an alternative method of using nano-suckers, a silicon wafer was covered with nano-silica crystals and ethoxylated trimethylolpropane triacrylate (ETPTA) via spin-coating, followed by coating with PVA and HCl solution. Thus, silica particles were embedded in a PVA film to create a positive PDMS replica mold mounted with nano-suckers for adhesion [164].

Aside from marine organisms, other forms of life on earth also provide inspiration for designing water-proof tissue adhesives. A wet adhesion skin patch from both amphibians (tree frogs) and the octopus has been manufactured [165]. The PMDS adhesion presented a surface pattern of octopus-like gibbous cups on a hexagonal structure (Figure 7c). The hexagonal micropatterns can adhere to the wet skin surface by draining liquid; meanwhile, the convex-shaped architecture can force liquid molecules into the inner chamber of the sucker to form a vacuum state, which induces a capillary-assisted suction effect to enhance normal adhesion strength on the wet substrate.

Inspired by growing tree roots interpenetrating into soil (Figure 5c), Liu *et al.* [166] developed high-adhesive, stretchable electrodes that were made from gold nanopiles and PDMS (Figure 7d). They fabricated gold nanopiles interlocked into PDMS substrates via interpenetration. The PDMS substrate can be glued to the target cylindrical wood surface by epoxy resin.

Moreover, inspired by the gecko foot pad, adhesive patches have been made from fibrillar arrays of micropatterned films. These patches can adhere to tissue via physical absorbance force in a chemical reaction-free scenario, which is safe and repeatable. In addition, the amphibian tree frogs also inspired the idea of two-phase (solid/liquid) adhesion. For example, a gel-like translucent adhesive was developed by dispersing PVDF spheres (~200 nm diameter) in PDMS [167]. PVDF spheres were chosen as the solid-phase because they have a large surface area and contain fluorine atoms that can bond with the contact surface via dipolar interactions. PDMS works as the liquid-phase due to the large elasticity of its polymer chain that can efficiently disperse the PVDF spheres and provide long-term stability. When compressed, the liquid phase (PDMS) allowed the solid spheres (PVDF) to flow onto the contact surface, increasing the contact area and strengthening the dipolar interactions with the contact surface.

A range of bioinspired or biomimetic adhesives with good performance are listed in Table 4. As with mussel-inspired adhesives, these bioinspired or biomimetic adhesives also exhibited excellent wet-adhesion ability [168–170]. As well as water-resistance, they exhibit reversible adhesion [162] and a switchable adhesion structure [171] due to their special mimicking structure. One adhesive with a microstructure surface could adhere tightly to targets by mimicking a mushroom shape [172]. Another adhesive,

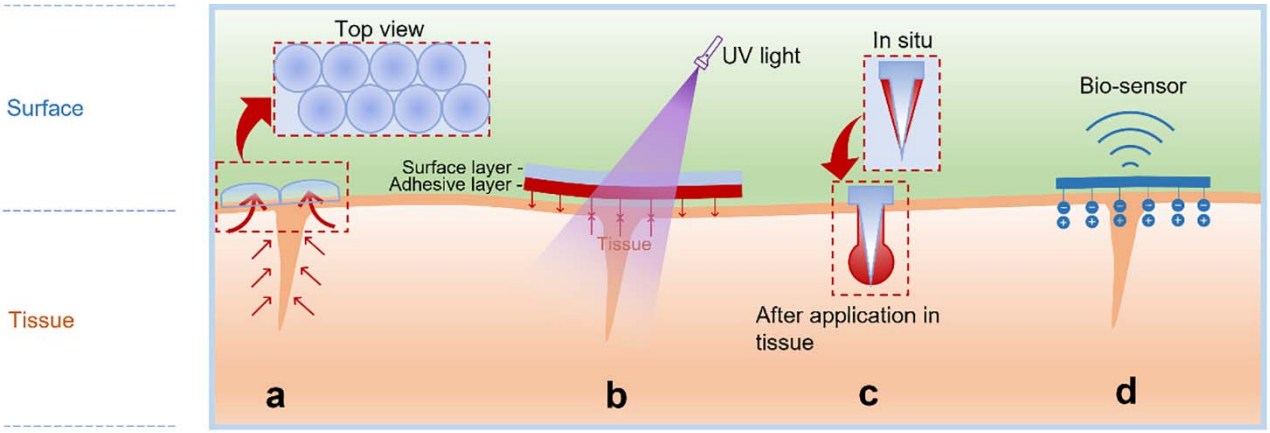

Figure 8. Future perspectives of tissue adhesives with multiple features: (**a**) repeatable adhesion; (**b**) one-side adhesion; (**c**) shape-memory adhesion; (**d**) adhesive-based electronics

bioinspired by a gecko foot, could glue tightly to a rough surface [173].

Future perspectives

Most tissue adhesives outperform traditional wound closure by sutures and staples. Having said that, there are limitations where underwater and bioactive diversity is concerned. In order to exploit adhesives with multiple functions, some extra features are worthy of mention, such as shape memory, controllable adhesion–cyclic adhesion and non-adhesion, one-side adhesion, adhesive electronics, and antibacterial and hemostasis adhesion, which will be a focus of future designs (Figure 8).

Shape memory adhesives Most adhesives, so far, are focused on the interfacial strength, anti-water ability [174], or adhesion time, cost etc [175]. From the perspective of biological evolution, tissue adhesives could also bear the smart nature of environmental-adaptive adhesion ability. Shape memory is the ability of materials to memorize their original shapes from a temporary deformed state under an external stimulus [176,177]. Adhesives can be designed with shape memory ability, e.g. as microneedles. As the microneedles penetrate through the epidermis into the dermis layer, they can change shape via contact with water (interstitial fluid) or temperature (body temperature), becoming firmly locked in the tissues. In this way, a moisture-induced microneedles-based adhesive patch can mechanically interlock with tissue. This patch contains swelling and non-swelling parts. Upon contact with physiological fluid, the volume change on one side leads to morphological transition and thus the needles become anchored inside (Figure 9a). [178] Smart needles may be laden with antibacterial agents or wound-healing regulators to promote tissue repair, or even biocompatible electronic materials to create a tissue-adhesive sensor to detect infection and control the healing process, temperature and pH on the wound bed [179–181]. Furthermore, the shape-memory adhesive can be designed for injured and bleeding organs with minimally invasive delivery. Instead of invasive surgery, an adhesive cardiac patch can be injected into the heart via a small orifice and return to its initial structure to form a firmly attached membrane after myocardial infarction [182].

Repeatable-adhesion adhesives Adhesives are generally functionalized for single use and not for repeatable purposes. After a first application, the performance of interfacial surface molecules will be compromised for the next use, e.g. covalent bonds are consumed and non-recoverable [50,86,108,183]. In order to address this concern, physical interaction is an alternative approach. For example, an octopus-inspired microsuckers-based wearable device can attach and detach cyclically on the skin by controlling the pressure, so that negative inner pressure results in adherence and detachment (Figure 9b) [50].

One-side adhesion One-side adhesion is an essential consideration when undesired tissue adherence is a concern. For example, in heart defect repairs, an adhesive cardiac patch may be undesirably glued to thorax tissue. We may design one-side-adhesion adhesives by simply grafting non-fouling and non-adhesive functional molecules to the other side for protection (Figure 9c) [49,184,185]. Tissue adhesives can work via photoinitiation and be activated by light exposure. Thus, Directional light (either UV or visible light) can be used to activate one side and achieve one-side adhesion.

Adhesives-based wearable electronics Consideration of integration between adhesives and bioelectronics allows us to consider a future image where biocompatible devices can take a foothold in tissues. Adhesives-based wearable electronics can be used to close wounds; on the other hand, they can be used to monitor healing processes in some essential body constituents, e.g. -brain, heart, blood vessel, nerves, skin, etc. Besides, through electronics, bio-electrics can mimic tissue and cell electrical signals, then tame cells for repairing or even

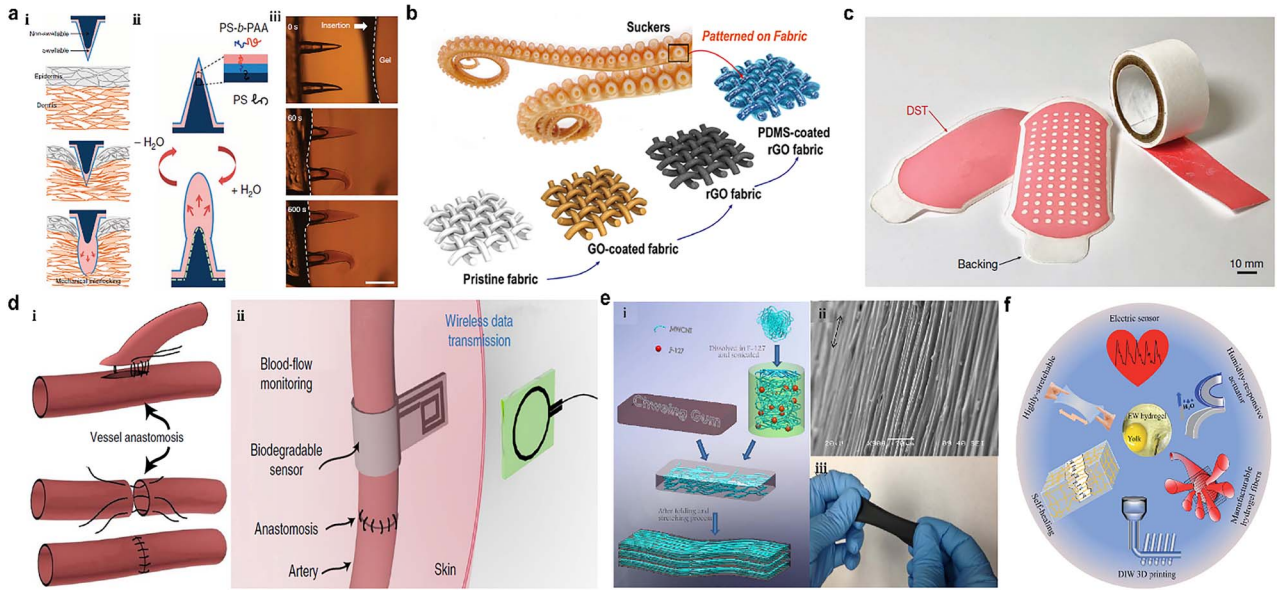

Figure 9. Future multifunctional tissue adhesives. (**a**) Swellable microneedle adhesive mechanically interlocks with tissue: (i) physical interlocking of water-induced shape-changing microneedle penetrating tissue; (ii) reversibly water responsive; (iii) time-dependent swelling of the microneedles on insertion into an agarose hydrogel. (Reprinted from ref. [178] with permission from Springer Nature Limited.) (**b**) rGO-coated polyurethane–polyester fabric and rGO-loaded PDMS wearable sensor. (Reprinted from ref. [190] with permission from the American Chemical Society.) (**c**) Double-sided adhesive tape with polyethylene-coated paper backing. (Reprinted from ref. [49] with permission from Springer Nature Limited.) (**d**) (i) Vessel anastomosis; and (ii) arterial blood flow monitored by the biosensor. (Reprinted from ref. [186] with permission from Springer Nature Limited.) (**e**) Attachable MWCNT-based gum sensor: (i) MWCNT-loaded gum membrane; (ii) SEM of membrane cross-section; (iii) optical image of the membrane. (Reprinted from ref. [187] with permission from the American Chemical Society.) (**f**) Wearable self-healing electronic hydrogel sensor made from natural egg white. (Reprinted from ref. [188] with permission from the Royal Society of Chemistry)

regenerating multifunctional organs. For example, a biosensor was designed to monitor blood flow after vessel anastomosis reconstructive surgery, in which the vessel patency could be detected in real time (Figure 9d) [186]. An adhesive-based biosensor could be designed for vessel anastomosis instead of suturing (Figure 9d(i)) and post-operative blood flow could also be monitored via this sensor (Figure 9d(ii)). In addition, such adhesive-based biosensors may be used in the future to detect body motion, e.g. by attaching them to skin or joints to sense muscle or joint motion (Figure 9e) [187]. Smart sensors have additional advantages e.g. wearable adhesive sensors with self-healing properties may solve breaking issues during the attachment/detachment process and in high-strain environments (Figure 9f) [188,189,190].

Conclusions

Despite a lot of research being carried out on tissue adhesives, there are no commercial products that meet all of the requirements, which leaves scope for future designs. When attempting to generate a nearly ideal tissue adhesive, the biggest challenge will be that it has characteristics that make it stand out from the others by possessing special qualities that means it can outperform all current products. We look forward to when multiple advanced tissue adhesives will become commercially available, in particular those that are simple and practical for surgeons, have greater adhesion abilities, smart attributes, underwater performance and that are flexible, permitting them to be altered on demand.

Authors contribution

Kaige Xu was responsible for the design and wrote the manuscript. Xiaozhuo Wu contributed to parts of the Figures drawing and revised the manuscript. Xingying Zhang provided suggestions. Malcolm Xing was responsible for the design and revised the manuscript. All authors read and approved the final manuscript.

Fundings

None.

Conflicts of interest

None declared.

References

1. Armitage J, Lockwood S. Skin incisions and wound closure. *Surgery (Oxford)*. 2011;29:496–501.
2. Cooney G, Kiernan A, Winter D, Simms C. Optimized wound closure using a biomechanical abdominal model. *Br J Surg*. 2018;105:395–400.
3. Kuo F, Lee D, Rogers GS. Prospective, randomized, blinded study of a new wound closure film versus cutaneous suture for surgical wound closure. *Dermatol Surg*. 2006;32:676–81.
4. Ghoreishian M, Gheisari R, Fayazi M. Tissue adhesive and suturing for closure of the surgical wound after removal of impacted mandibular third molars: a comparative study. *Oral Surg Oral Med Oral Pathol Oral Radiol Endod*. 2009;108:e14–6.
5. Artzi N. Sticking with the pattern for a safer glue. *Sci Transl Med*. 2013;5:205ec161–1.

6. George W. Suturing or stapling in gastrointestinal surgery: a prospective randomized study. *Br J Surg*. 1991;78: 337–41.
7. Pai D, Shenoy R, Chethan K. Comparison of non-absorbable (polypropylene) versus delayed absorbable (polydioxanone) suture material for abdominal wound closure after laparotomy. *Int Surg J*. 2018;5:1690–6.
8. Takayama S, Yamamoto T, Tsuchiya C, Noguchi H, Sato J, Ishii Y. Comparing Steri-strip and surgical staple wound closures after primary total knee arthroplasties. *Eur J Orthop Surg Traumatol*. 2017;27:113–8.
9. Katz S, Izhar M, Mirelman D. Bacterial adherence to surgical sutures. A possible factor in suture induced infection. *Ann Surg*. 1981;194:35.
10. Galal I, El-Hindawy K. Impact of using triclosan-antibacterial sutures on incidence of surgical site infection. *Am J Surg*. 2011;202:133–8.
11. Bruce J, Krukowski ZH, Al-Khairy G, Russell EM, Park K. Systematic review of the definition and measurement of anastomotic leak after gastrointestinal surgery. *Br J Surg*. 2001; 88:1157–68.
12. Essani R, Bergamaschi R. Anastomotic leak in colorectal surgery: a review. *Gastroentero Pl/Gastroentero*. 2009;16: 123–7.
13. Cai W, Shen K, Ji P, Jia Y, Han S, Zhang W, *et al.* The notch pathway attenuates burn-induced acute lung injury in rats by repressing reactive oxygen species. *Burns Trauma*. 2022;10:tkac008. https://doi.org/10.1093/burnst/tkac008.
14. Donkerwolcke M, Burny F, Muster D. Tissues and bone adhesives—historical aspects. *Biomaterials*. 1998;19:1461–6.
15. Mehdizadeh M, Yang J. Design strategies and applications of tissue bioadhesives. *Macromol Biosci*. 2013;13:271–88.
16. Vakalopoulos KA, Daams F, Wu Z, Timmermans L, Jeekel JJ, Kleinrensink G-J, *et al.* Tissue adhesives in gastrointestinal anastomosis: a systematic review. *J Surg Res*. 2013;180: 290–300.
17. Chen S, Zhang M, Shao X, Wang X, Zhang L, Xu P, *et al.* A laminin mimetic peptide SIKVAV-conjugated chitosan hydrogel promoting wound healing by enhancing angiogenesis, re-epithelialization and collagen deposition. *J Mater Chem B*. 2015;3:6798–804.
18. Guo Y, Wang Y, Zhao X, Li X, Wang Q, Zhong W, *et al.* Snake extract-laden hemostatic bioadhesive gel cross-linked by visible light. *Sci Adv*. 2021;7:eabf9635. https://doi.10.1126/sciadv.abf9635.
19. Xu K, Chang Q, Liu Y, Xing M. In: Bingyun Li, Thomas Fintan Moriarty, Thomas Webster, Malcolm Xing (eds). *Recent Physical Interaction-based Bioadhesives*. New York City, US: Racing for the Surface: Springer, 2020, 693–721.
20. Cronkite EP, Lozner EL, Deaver JM. Use of thrombin and fibrinogen in skin grafting: preliminary report. *JAMA*. 1944;124:976–8.
21. Bré LP, Zheng Y, Pêgo AP, Wang W. Taking tissue adhesives to the future: from traditional synthetic to new biomimetic approaches. *Biomater Sci*. 2013;1:239–53.
22. Chen Y, Cheng W, Teng L, Jin M, Lu B, Ren L, *et al.* Graphene oxide hybrid supramolecular hydrogels with self-healable, bioadhesive and stimuli-responsive properties and drug delivery application. *Macromol Mater Eng*. 2018;303:1700660. https://doi.org/10.1002/mame.201700660.
23. Spotnitz W. In: David H Sierra, Renato Saltz (des). *History of tissue adhesive*. Lancaster, PA: Technomic Publishing Co., Inc., 1996.
24. Li X, Zhou J, Liu Z, Chen J, Lü S, Sun H, *et al.* A PNIPAAm-based thermosensitive hydrogel containing SWCNTs for stem cell transplantation in myocardial repair. *Biomaterials*. 2014;35:5679–88.
25. Ayyıldız SN, Ayyıldız A. Cyanoacrylic tissue glues: biochemical properties and their usage in urology. *Turk J Urol*. 2017;43: 14–24.
26. Bravo-Osuna I, Vauthier C, Farabollini A, Palmieri GF, Ponchel G. Mucoadhesion mechanism of chitosan and thiolated chitosan-poly (isobutyl cyanoacrylate) core-shell nanoparticles. *Biomaterials*. 2007;28:2233–43.
27. Nicolas J, Vauthier C. In: Wang DO, Packwood D (ed). *Poly (Alkyl Cyanoacrylate) Nanosystems*. New York City, US: Intracellular Delivery: Springer, 2011, 225–50.
28. Ritterband DC, Meskin SW, Shapiro DE, Kusmierczyk J, Seedor JA, Koplin RS. Laboratory model of tissue adhesive (2-octyl cyanoacrylate) in sealing clear corneal cataract wounds. *Am J Ophthalmol*. 2005;140:1039–43.
29. Leggat PA, Smith DR, Kedjarune U. Surgical applications of cyanoacrylate adhesives: a review of toxicity. *ANZ J Surg*. 2007;77:209–13.
30. Singer AJ, Quinn JV, Hollander JE. The cyanoacrylate topical skin adhesives. *Am J Emerg Med*. 2008;26:490–6.
31. Yu P, Zhong W. Hemostatic materials in wound care. *Burns Trauma*. 2021;9:tkab019. https://doi.org/10.1093/burnst/tkab019.
32. Janmey PA, Winer JP, Weisel JW. Fibrin gels and their clinical and bioengineering applications. *J R Soc Interface*. 2009;6:1–10.
33. Radosevich M, Goubran H, Burnouf T. Fibrin sealant: scientific rationale, production methods, properties, and current clinical use. *Vox Sang*. 1997;72:133–43.
34. Petersen BT, Barkun A, Carpenter S, Chotiprasidhi P, Chuttani R, Silverman W, *et al.* Tissue adhesives and fibrin glues: November 2003. *Gastrointest Endosc*. 2004;60:327–33.
35. Pescatore P, Verbeke C, Härle M, Manegold B. Fibrin sealing in peptic ulcer bleeding: the fate of the clot. *Endoscopy*. 1998;30:519–23.
36. Nistor RF, Chiari FM, Maier H, Hehl K. The fixed combination of collagen with components of fibrin adhesive-a new hemostypic agent in skull base procedures. *Skull Base Surg*. 1997;7:23–30.
37. Caers J, Reekmans A, Jochmans K, Naegels S, Mana F, Urbain D, *et al.* Factor V inhibitor after injection of human thrombin (tissucol) into a bleeding peptic ulcer. *Endoscopy*. 2003;35:542–4.
38. Flahiff C, Feldman D, Saltz R, Huang S. Mechanical properties of fibrin adhesives for blood vessel anastomosis. *J Biomed Mater Res*. 1992;26:481–91.
39. Braunwald NS, Gay W, Tatooles CJ. Evaluation of crosslinked gelatin as a tissue adhesive and hemostatic agent: an experimental study. *Surgery*. 1966;59:1024–30.
40. Nomori H, Horio H. Gelatin-resorcinol–formaldehyde-glutaraldehyde glue-spread stapler prevents air leakage from the lung. *Ann Thorac Surg*. 1997;63:352–5.
41. Matsuda S, Iwata H, Se N, Ikada Y. Bioadhesion of gelatin films crosslinked with glutaraldehyde. *J Biomed Mater Res J*

Soc Biomater Jap Soc Biomater Austr Soc Biomater. 1999;45:20–7.
42. Chang MC, Ko C-C, Douglas WH. Conformational change of hydroxyapatite/gelatin nanocomposite by glutaraldehyde. *Biomaterials*. 2003;24:3087–94.
43. Nomori H, Horio H, Morinaga S, Suemasu K. Gelatin-resorcinol–formaldehyde-glutaraldehyde glue for sealing pulmonary air leaks during thoracoscopic operation. *Ann Thorac Surg*. 1999;67:212–6.
44. Bhatia SK. *Biomaterials for clinical applications*. Germany: Springer New York, 2010.
45. Chao HH, Torchiana DF. BioGlue: albumin/glutaraldehyde sealant in cardiac surgery. *J Card Surg*. 2003;18:500–3.
46. Fürst W, Banerjee A. Release of glutaraldehyde from an albumin-glutaraldehyde tissue adhesive causes significant in vitro and in vivo toxicity. *Ann Thorac Surg*. 2005;79:1522–8.
47. Gruber-Blum S, Petter-Puchner A, Mika K, Brand J, Redl H, Öhlinger W, *et al*. A comparison of a bovine albumin/glutaraldehyde glue versus fibrin sealant for hernia mesh fixation in experimental onlay and IPOM repair in rats. *Surg Endosc*. 2010;24:3086–94.
48. Li J, Celiz A, Yang J, Yang Q, Wamala I, Whyte W, *et al*. Tough adhesives for diverse wet surfaces. *Science*. 2017;357:378–81.
49. Yuk H, Varela CE, Nabzdyk CS, Mao X, Padera RF, Roche ET, *et al*. Dry double-sided tape for adhesion of wet tissues and devices. *Nature*. 2019;575:169–74.
50. Liu C, Liu X, Liu C, Wang N, Chen H, Yao W, *et al*. A highly efficient, in situ wet-adhesive dextran derivative sponge for rapid hemostasis. *Biomaterials*. 2019;205:23–37.
51. Fan C, Xu K, Huang Y, Liu S, Wang T, Wang W, *et al*. Viscosity and degradation controlled injectable hydrogel for esophageal endoscopic submucosal dissection. *Bioact Mater*. 2020;6:1150–62.
52. Bui R, Brook MA. Dynamic covalent Schiff-base silicone polymers and elastomers. *Polymer*. 2019;160:282–90.
53. Ren H, Zhao F, Zhang Q, Huang X, Wang Z. Autophagy and skin wound healing. *Burns Trauma*. 2022;10:tkac003. https://doi.org/10.1093/burnst/tkac003.
54. Artzi N, Shazly T, Baker AB, Bon A, Edelman ER. Aldehyde-amine chemistry enables modulated biosealants with tissue-specific adhesion. *Adv Mater*. 2009;21:3399–403.
55. Liu J, Li J, Yu F, Zhao Y-x. Mo X-m, Pan J-f. In situ forming hydrogel of natural polysaccharides through Schiff base reaction for soft tissue adhesive and hemostasis. *Int J Biol Macromol*. 2020;147:653–66.
56. Hong Y, Zhou F, Hua Y, Zhang X, Ni C, Pan D, *et al*. A strongly adhesive hemostatic hydrogel for the repair of arterial and heart bleeds. *Nat Commun*. 2019;10:1–11.
57. Shao C, Wang M, Meng L, Chang H, Wang B, Xu F, *et al*. Mussel-inspired cellulose nanocomposite tough hydrogels with synergistic self-healing, adhesive, and strain-sensitive properties. *Chem Mater*. 2018;30:3110–21.
58. Dong H, Li Q, Cao X. A medical adhesive used in wet environment by blending tannic acid and silk fibroin. *Biomater Sci*. 2020;8:2694–701.
59. Kim S-H, Kim K, Kim BS, An Y-H, Lee U-J, Lee S-H, *et al*. Fabrication of polyphenol-incorporated anti-inflammatory hydrogel via high-affinity enzymatic crosslinking for wet tissue adhesion. *Biomaterials*. 2020;242:119905. https://doi.10.1016/j.biomaterials.2020.119905.
60. An Y-H, Kim HD, Kim K, Lee S-H, Yim H-G, Kim B-G, *et al*. Enzyme-mediated tissue adhesive hydrogels for meniscus repair. *Int J Biol Macromol*. 2018;110:479–87.
61. Liu B, Wang Y, Miao Y, Zhang X, Fan Z, Singh G, *et al*. Hydrogen bonds autonomously powered gelatin methacrylate hydrogels with super-elasticity, self-heal and underwater self-adhesion for sutureless skin and stomach surgery and E-skin. *Biomaterials*. 2018;171:83–96.
62. Bet M, Goissis G, Vargas S, Selistre-de-Araujo H. Cell adhesion and cytotoxicity studies over polyanionic collagen surfaces with variable negative charge and wettability. *Biomaterials*. 2003;24:131–7.
63. Rao P, Sun TL, Chen L, Takahashi R, Shinohara G, Guo H, *et al*. Tough hydrogels with fast, strong, and reversible underwater adhesion based on a multiscale design. *Adv Mater*. 2018;30:1801884. http://doi.10.1002/adma.201801884.
64. Roy CK, Guo HL, Sun TL, Ihsan AB, Kurokawa T, Takahata M, *et al*. Self-adjustable adhesion of Polyampholyte hydrogels. *Adv Mater*. 2015;27:7344–8.
65. Cui C, Wu T, Gao F, Fan C, Xu Z, Wang H, *et al*. An autolytic high strength instant adhesive hydrogel for emergency self-rescue. *Adv Funct Mater*. 2018;28:1804925. https://doi.org/10.1002/adfm.201804925.
66. Xu K, Liu Y, Bu S, Wu T, Chang Q, Singh G, *et al*. Egg albumen as a fast and strong medical adhesive glue. *Adv Healthc Mater*. 2017;6:1700132. https://doi.org/10.1002/adhm.201700132.
67. Ghobril C, Grinstaff M. The chemistry and engineering of polymeric hydrogel adhesives for wound closure: a tutorial. *Chem Soc Rev*. 2015;44:1820–35.
68. Oliveira NM, Zhang YS, Ju J, Chen A-Z, Chen Y, Sonkusale SR, *et al*. Hydrophobic hydrogels: toward construction of floating (bio) microdevices. *Chem Mater*. 2016;28:3641–8.
69. Lih E, Lee JS, Park KM, Park KD. Rapidly curable chitosan–PEG hydrogels as tissue adhesives for hemostasis and wound healing. *Acta Biomater*. 2012;8:3261–9.
70. Yu F, Cao X, Du J, Wang G, Chen X. Multifunctional hydrogel with good structure integrity, self-healing, and tissue-adhesive property formed by combining Diels–Alder click reaction and acylhydrazone bond. *ACS Appl Mater Interfaces*. 2015;7:24023–31.
71. Faghihnejad A, Feldman KE, Yu J, Tirrell MV, Israelachvili JN, Hawker CJ, *et al*. Adhesion and surface interactions of a self-healing polymer with multiple hydrogen-bonding groups. *Adv Funct Mater*. 2014;24:2322–33.
72. Dankers PY, Harmsen MC, Brouwer LA, Van Luyn MJ, Meijer E. A modular and supramolecular approach to bioactive scaffolds for tissue engineering. *Nat Mater*. 2005;4:568–74.
73. Wang H, Liu Y, Cai K, Zhang B, Tang S, Zhang W, *et al*. Antibacterial polysaccharide-based hydrogel dressing containing plant essential oil for burn wound healing. *Burns Trauma*. 2021;9:tkab041. https://doi.org/10.1093/burnst/tkab041.
74. Miyamoto M, Sasakawa S, Ozawa T, Kawaguchi H, Ohtsuka Y. Platelet aggregation induced by latex particles: I. effects of size, surface potential and hydrophobicity of particles. *Biomaterials*. 1989;10:251–7.
75. Dumas JJ, Kumar R, Seehra J, Somers WS, Mosyak L. Crystal structure of the GpIbα-thrombin complex essential for platelet aggregation. *Science*. 2003;301:222–6.

76. Chen X, Taguchi T. Enhanced skin adhesive property of hydrophobically modified poly (vinyl alcohol) films. *ACS Omega*. 2020;5:1519–27.
77. Zhang D, Xu Z, Li H, Fan C, Cui C, Wu T, *et al.* Fabrication of strong hydrogen-bonding induced coacervate adhesive hydrogels with antibacterial and hemostatic activities. *Biomater Sci*. 2020;8:1455–63.
78. Yang H, Li C, Tang J, Suo Z. Strong and degradable adhesion of hydrogels. *ACS Appl Bio Mater*. 2019;2:1781–6.
79. Yang J, Bai R, Li J, Yang C, Yao X, Liu Q, *et al.* Design molecular topology for wet–dry adhesion. *ACS Appl Mater Interfaces*. 2019;11:24802–11.
80. Mooney DJ, Silva EA. A glue for biomaterials. *Nat Mater*. 2007;6:327–8.
81. Xu L, Gao S, Zhou R, Zhou F, Qiao Y, Qiu D. Bioactive pore-forming bone adhesives facilitating cell ingrowth for fracture healing. *Adv Mater*. 2020;32:1907491. https://doi.org/10.1002/adma.201907491.
82. Liu J, Lin S, Liu X, Qin Z, Yang Y, Zang J, *et al.* Fatigue-resistant adhesion of hydrogels. *Nat Commun*. 2020;11:1–9.
83. Dompé M, Cedano-Serrano FJ, Heckert O, van den Heuvel N, van der Gucht J, Tran Y, *et al.* Thermoresponsive complex Coacervate-based underwater adhesive. *Adv Mater*. 2019;31:1808179. https://doi.org/10.1002/adma.201808179.
84. Ryplida B, Lee KD, In I, Park SY. Light-induced swelling-responsive conductive, adhesive, and stretchable wireless film hydrogel as electronic artificial skin. *Adv Funct Mater*. 2019;29:1903209. https://doi.org/10.1002/adfm.201903209.
85. Davidson MD, Ban E, Schoonen AC, Lee MH, D'Este M, Shenoy VB, *et al.* Mechanochemical adhesion and plasticity in multifiber hydrogel networks. *Adv Mater*. 2020;32:1905719. https://doi.org/10.1002/adma.201905719.
86. Gonzalez MA, Simon JR, Ghoorchian A, Scholl Z, Lin S, Rubinstein M, *et al.* Strong, tough, stretchable, and self-adhesive hydrogels from intrinsically unstructured proteins. *Adv Mater*. 2017;29:1604743. https://doi.org/10.1002/adma.201604743.
87. Bu Y, Zhang L, Sun G, Sun F, Liu J, Yang F, *et al.* Tetra-PEG based hydrogel sealants for In vivo visceral Hemostasis. *Adv Mater*. 2019;31:1901580. https://doi.org/10.1002/adma.201901580.
88. Tan H, Jin D, Qu X, Liu H, Chen X, Yin M, *et al.* A PEG-lysozyme hydrogel harvests multiple functions as a fit-to-shape tissue sealant for internal-use of body. *Biomaterials*. 2019;192:392–404.
89. Shagan A, Zhang W, Mehta M, Levi S, Kohane DS, Mizrahi B. Hot glue gun releasing biocompatible tissue adhesive. *Adv Funct Mater*. 2020;30:1900998. https://doi.org/10.1002/adfm.201900998.
90. Zhao X, Liang Y, Huang Y, He J, Han Y, Guo B. Physical double-network hydrogel adhesives with rapid shape adaptability, fast self-healing, antioxidant and NIR/pH stimulus-responsiveness for multidrug-resistant bacterial infection and removable wound dressing. *Adv Funct Mater*. 2020;30:1910748. https://doi.org/10.1002/adfm.201910748.
91. Seo JW, Kim H, Kim K, Choi SQ, Lee HJ. Calcium-modified silk as a biocompatible and strong adhesive for epidermal electronics. *Adv Funct Mater*. 2018;28:1800802. https://doi.org/10.1002/adfm.201800802.
92. Granskog V, García-Gallego S, von Kieseritzky J, Rosendahl J, Stenlund P, Zhang Y, *et al.* High-performance thiol–Ene composites unveil a new era of adhesives suited for bone repair. *Adv Funct Mater*. 2018;28:1800372. https://doi.org/10.1002/adfm.201870180.
93. Li B, Whalen JJ, Humayun MS, Thompson ME. Reversible bioadhesives using tannic acid primed thermally-responsive polymers. *Adv Funct Mater*. 2020;30:1907478. https://doi.org/10.1002/adfm.201907478.
94. Liu X, Zhang Q, Duan L, Gao G. Tough adhesion of nucleobase-Tackifed gels in diverse solvents. *Adv Funct Mater*. 2019;29:1900450. https://doi.org/10.1002/adfm.201900450.
95. Gang H, Liang C. Biological activity of biomimetic dermal papilla spheres prepared by culture of dermal papilla cells of mice based on hanging drops of gelatin methacrylate and its hair-inducing function in nude mice. *Zhonghua Shaoshang Zazhi*. 2021;37:770–80.
96. Sani ES, Kheirkhah A, Rana D, Sun Z, Foulsham W, Sheikhi A, *et al.* Sutureless repair of corneal injuries using naturally derived bioadhesive hydrogels. *Sci Adv*. 2019;5:eaav1281. http://doi.10.1126/sciadv.aav1281.
97. Assmann A, Vegh A, Ghasemi-Rad M, Bagherifard S, Cheng G, Sani ES, *et al.* A highly adhesive and naturally derived sealant. *Biomaterials*. 2017;140:115–27.
98. Annabi N, Zhang Y-N, Assmann A, Sani ES, Cheng G, Lassaletta AD, *et al.* Engineering a highly elastic human protein–based sealant for surgical applications. *Sci Transl Med*. 2017;9:eaai7466. http://doi.10.1126/scitranslmed.aai7466. Erratum in: Sci Transl Med. 2018 Dec 5;10(470): PMID: 28978753.
99. Blacklow S, Li J, Freedman B, Zeidi M, Chen C, Mooney D. Bioinspired mechanically active adhesive dressings to accelerate wound closure. *Sci Adv*. 2019;5:eaaw3963. http://doi.10.1126/sciadv.aaw3963.
100. Yang J, Bai R, Suo Z. Topological adhesion of wet materials. *Adv Mater*. 2018;30:1800671. https://doi.org/10.1002/adma.201800671.
101. Thavarajah D, De Lacy P, Hussain R, Redfern RM. Post-operative cervical cord compression induced by hydrogel (DuraSeal): a possible complication. *Spine*. 2010;35:E25–6. http://doi.10.1097/BRS.0b013e3181b9fc45.
102. Mehdizadeh M, Weng H, Gyawali D, Tang L, Yang J. Injectable citrate-based mussel-inspired tissue bioadhesives with high wet strength for sutureless wound closure. *Biomaterials*. 2012;33:7972–83.
103. Wang L, Liu Y, Ye G, He Y, Li B, Guan Y, *et al.* Injectable and conductive cardiac patches repair infarcted myocardium in rats and minipigs. *Nat Biomed Eng*. 2021;5:1157–73.
104. Du X, Hou Y, Wu L, Li S, Yu A, Kong D, *et al.* Anti-infective hydrogel adhesive with non-swelling and robust mechanical properties for Sutureless wound closure. *J Mater Chem B*. 2020;8:5682–93.
105. Barrett DG, Bushnell GG, Messersmith PB. Mechanically robust, negative-swelling, mussel-inspired tissue adhesives. *Adv Healthc Mater*. 2013;2:745–55.
106. Rose S, Prevoteau A, Elzière P, Hourdet D, Marcellan A, Leibler L. Nanoparticle solutions as adhesives for gels and biological tissues. *Nature*. 2014;505:382–5.
107. Lu X, Shi S, Li H, Gerhard E, Lu Z, Tan X, *et al.* Magnesium oxide-crosslinked low-swelling citrate-based mussel-inspired tissue adhesives. *Biomaterials*. 2020;232:119719. https://doi.org/10.1016/j.biomaterials.2019.119719.
108. Inoue A, Yuk H, Lu B, Zhao X. Strong adhesion of wet conducting polymers on diverse substrates. *Sci Adv*. 2020;6:eaay5394. http://doi.10.1126/sciadv.aay5394.

109. Costa RR, da Costa DS, Reis RL, Pashkuleva I. Bioinspired baroplastic glycosaminoglycan sealants for soft tissues. *Acta Biomater*. 2019;87:108–17.
110. Zhao Q, Lee DW, Ahn BK, Seo S, Kaufman Y, Israelachvili JN, *et al*. Underwater contact adhesion and microarchitecture in polyelectrolyte complexes actuated by solvent exchange. *Nat Mater*. 2016;15:407–12.
111. Ryu JH, Kim HJ, Kim K, Yoon G, Wang Y, Choi GS, *et al*. Multipurpose intraperitoneal adhesive patches. *Adv Funct Mater*. 2019;29:1900495. https://doi.org/10.1002/adfm.201900495.
112. Gill SK, Roohpour N, Topham PD, Tighe BJ. Tunable denture adhesives using biomimetic principles for enhanced tissue adhesion in moist environments. *Acta Biomater*. 2017;63:326–35.
113. Pan Z, Zhang K-R, Gao H-L, Zhou Y, Yan B-B, Yang C, *et al*. Activating proper inflammation for wound-healing acceleration via mesoporous silica nanoparticle tissue adhesive. *Nano Res*. 2020;13:373–9.
114. Okada M, Hara ES, Yabe A, Okada K, Shibata Y, Torii Y, *et al*. Titanium as an instant adhesive for biological soft tissue. *Adv Mater Interfaces*. 2020;7:1902089. https://doi.org/10.1002/admi.201902089.
115. Yang K, Wang Y, You Y, Yang H, Hao X. Non-equilibrium polymerization enables adhesive material with anti-freezing, multipurpose adhesion, long-term air stability and anisotropic deformation. *Chem Eng J*. 2020;382:122926. https://doi.org/10.1016/j.cej.2019.122926.
116. Gao Y, Wu K, Suo Z. Photodetachable adhesion. *Adv Mater*. 2019;31:1806948. https://doi.org/10.1002/adma.201806948.
117. Walker BW, Lara RP, Yu CH, Sani ES, Kimball W, Joyce S, *et al*. Engineering a naturally-derived adhesive and conductive cardiopatch. *Biomaterials*. 2019;207:89–101.
118. Yi H, Seong M, Sun K, Hwang I, Lee K, Cha C, *et al*. Wet-responsive, reconfigurable, and biocompatible hydrogel adhesive films for transfer printing of Nanomembranes. *Adv Funct Mater*. 2018;28:1706498. https://doi.org/10.1002/adfm.201706498.
119. Yang H, Li C, Yang M, Pan Y, Yin Q, Tang J, *et al*. Printing hydrogels and elastomers in arbitrary sequence with strong adhesion. *Adv Funct Mater*. 2019;29:1901721. https://doi.org/10.1002/adfm.201901721.
120. Ge L, Li Q, Huang Y, Yang S, Ouyang J, Bu S, *et al*. Polydopamine-coated paper-stack nanofibrous membranes enhancing adipose stem cells' adhesion and osteogenic differentiation. *J Mater Chem B*. 2014;2:6917–23.
121. Zhang S, Xu K, Darabi MA, Yuan Q, Xing M. Mussel-inspired alginate gel promoting the osteogenic differentiation of mesenchymal stem cells and anti-infection. *Mater Sci Eng C*. 2016;69:496–504.
122. Hsu HH, Liu Y, Wang Y, Li B, Luo G, Xing M, *et al*. Mussel-inspired autonomously self-healable all-in-one supercapacitor with biocompatible hydrogel. *ACS Sustain Chem Eng*. 2020;8:6935–48.
123. Wang L, Zhang X, He Y, Wang Y, Zhong W, Mequanint K, *et al*. Ultralight conductive and elastic aerogel for skeletal muscle atrophy regeneration. *Adv Funct Mater*. 2019;29:1806200. https://doi.org/10.1002/adfm.201806200.
124. Song C, Zhang X, Wang L, Wen F, Xu K, Xiong W, *et al*. An injectable conductive three-dimensional elastic network by tangled surgical-suture spring for heart repair. *ACS Nano*. 2019;13:14122–37.
125. Zhang S, Xu K, Ge L, Darabi MA, Xie F, Derakhshanfar S, *et al*. A novel nano-silver coated and hydrogel-impregnated polyurethane nanofibrous mesh for ventral hernia repair. *RSC Adv*. 2016;6:90571–8.
126. Xu H, Zhang G, Xu K, Wang L, Yu L, Xing MM, *et al*. Mussel-inspired dual-functional PEG hydrogel inducing mineralization and inhibiting infection in maxillary bone reconstruction. *Mater Sci Eng C*. 2018;90:379–86.
127. Han L, Liu K, Wang M, Wang K, Fang L, Chen H, *et al*. Mussel-inspired adhesive and conductive hydrogel with long-lasting moisture and extreme temperature tolerance. *Adv Funct Mater*. 2018;28:1704195. http://doi.10.1002/adfm.201704195.
128. Liao M, Wan P, Wen J, Gong M, Wu X, Wang Y, *et al*. Wearable, healable, and adhesive epidermal sensors assembled from mussel-inspired conductive hybrid hydrogel framework. *Adv Funct Mater*. 2017;27:1703852. https://doi.org/10.1002/adfm.201703852.
129. Salzlechner C, Haghighi T, Huebscher I, Walther AR, Schell S, Gardner A, *et al*. Adhesive hydrogels for maxillofacial tissue regeneration using minimally invasive procedures. *Adv Healthc Mater*. 2020;9:1901134. https://doi.org/10.1002/adhm.201901134.
130. Ruprai H, Shanu A, Mawad D, Hook JM, Kilian K, George L, *et al*. Porous chitosan adhesives with L-DOPA for enhanced photochemical tissue bonding. *Acta Biomater*. 2020;101:314–26.
131. Jiang J, Wan W, Ge L, Bu S, Zhong W, Xing M. Mussel-inspired nanofibrous sheet for suture-less stomach incision surgery. *Chem Commun*. 2015;51:8695–8.
132. Wang L, Jiang J, Hua W, Darabi A, Song X, Song C, *et al*. Mussel-inspired conductive cryogel as cardiac tissue patch to repair myocardial infarction by migration of conductive nanoparticles. *Adv Funct Mater*. 2016;26:4293–305.
133. Jiang P, Li S, Lai J, Zheng H, Lin C, Shi P, *et al*. Nanoparticle-programmed surface for drug release and cell regulation via reversible hybridization reaction. *ACS Appl Mater Interfaces*. 2017;9:4467–74.
134. Wu T, Cui C, Huang Y, Liu Y, Fan C, Han X, *et al*. Coadministration of an adhesive conductive hydrogel patch and an injectable hydrogel to treat myocardial infarction. *ACS Appl Mater Interfaces*. 2019;12:2039–48.
135. Han L, Lu X, Liu K, Wang K, Fang L, Weng L-T, *et al*. Mussel-inspired adhesive and tough hydrogel based on nanoclay confined dopamine polymerization. *ACS Nano*. 2017;11:2561–74.
136. Cui C, Fan C, Wu Y, Xiao M, Wu T, Zhang D, *et al*. Water-triggered Hyperbranched polymer universal adhesives: from strong underwater adhesion to rapid sealing Hemostasis. *Adv Mater*. 2019;31:1905761. https://doi.org/10.1002/adma.201905761.
137. Waite JH. Mussel adhesion–essential footwork. *J Exp Biol*. 2017;220:517–30.
138. Ahn BK. Perspectives on mussel-inspired wet adhesion. *J Am Chem Soc*. 2017;139:10166–71.
139. Jiang J, Huang Y, Wang Y, Xu H, Xing M, Zhong W. Mussel-inspired dopamine and carbon nanotube leading to a biocompatible self-rolling conductive hydrogel film. *Materials*. 2017;10:964. https://doi.org/10.3390/ma10080964.
140. Yu J, Wei W, Danner E, Ashley RK, Israelachvili JN, Waite JH. Mussel protein adhesion depends on interprotein thiol-mediated redox modulation. *Nat Chem Biol*. 2011;7:588–90.

141. Wei K, Senturk B, Matter MT, Wu X, Herrmann IK, Rottmar M, *et al.* Mussel-inspired injectable hydrogel adhesive formed under mild conditions features near-native tissue properties. *ACS Appl Mater Interfaces*. 2019;11:47707–19.
142. Gebbie MA, Wei W, Schrader AM, Cristiani TR, Dobbs HA, Idso M, *et al.* Tuning underwater adhesion with cation–π interactions. *Nat Chem*. 2017;9:473–9.
143. Tiu BDB, Delparastan P, Ney MR, Gerst M, Messersmith PB. Enhanced adhesion and cohesion of bioinspired dry/wet pressure-sensitive adhesives. *ACS Appl Mater Interfaces*. 2019; 11:28296–306.
144. Lee D, Bae H, Ahn J, Kang T, Seo D-G, Hwang DS. Catechol-thiol-based dental adhesive inspired by underwater mussel adhesion. *Acta Biomater*. 2020;103:92–101.
145. Deepankumar K, Lim C, Polte I, Zappone B, Labate C, De Santo MP, *et al.* Supramolecular β-sheet suckerin–based underwater adhesives. *Adv Funct Mater*. 2020;30:1907534. https://doi.org/10.1002/adfm.201907534.
146. Massoumi B, Abbasian M, Jahanban-Esfahlan R, Mohammad-Rezaei R, Khalilzadeh B, Samadian H, *et al.* A novel bioinspired conductive, biocompatible, and adhesive terpolymer based on polyaniline, polydopamine, and polylactide as scaffolding biomaterial for tissue engineering application. *Int J Biol Macromol*. 2020;147:1174–84.
147. Li S, Chen N, Li Y, Zhao J, Hou X, Yuan X. Environment-dependent adhesive Behaviors of mussel-inspired coordinate-crosslinked bioadhesives. *Macromol Mater Eng*. 2020; 305:1900620. https://doi.org/10.1002/mame.201900620.
148. Seo S, Lee DW, Ahn JS, Cunha K, Filippidi E, Ju SW, *et al.* Significant performance enhancement of polymer resins by bioinspired dynamic bonding. *Adv Mater*. 2017;29:1703026. https://doi.org/10.1002/adma.201703026.
149. Han L, Wang M, Li P, Gan D, Yan L, Xu J, *et al.* Mussel-inspired tissue-adhesive hydrogel based on the polydopamine–chondroitin sulfate complex for growth-factor-free cartilage regeneration. *ACS Appl Mater Interfaces*. 2018;10: 28015–26.
150. Cheng H, Yue K, Kazemzadeh-Narbat M, Liu Y, Khalilpour A, Li B, *et al.* Mussel-inspired multifunctional hydrogel coating for prevention of infections and enhanced osteogenesis. *ACS Appl Mater Interfaces*. 2017;9:11428–39.
151. Higginson CJ, Malollari KG, Xu Y, Kelleghan AV, Ricapito NG, Messersmith PB. Bioinspired design provides high-strength benzoxazine structural adhesives. *Angew Chem*. 2019; 131:12399–407.
152. Jeon EY, Lee J, Kim BJ, Joo KI, Kim KH, Lim G, *et al.* Bio-inspired swellable hydrogel-forming double-layered adhesive microneedle protein patch for regenerative internal/external surgical closure. *Biomaterials*. 2019;222:119439. https://doi.org/10.1016/j.biomaterials.2019.119439.
153. Hong S, Pirovich D, Kilcoyne A, Huang CH, Lee H, Weissleder R. Supramolecular Metallo-bioadhesive for minimally invasive use. *Adv Mater*. 2016;28:8675–80.
154. Huang N, Liu Y, Fang Y, Zheng S, Wu J, Wang M, *et al.* Gold nanoparticles induce tumor vessel normalization and impair metastasis by inhibiting endothelial Smad2/3 Signaling. *ACS Nano*. 2020;14:7940–58.
155. Wilker JJ. Materials science: how to suck like an octopus. *Nature*. 2017;546:358–9.
156. Chen R, Fu Q, Liu Z, Hu X, Liu M, Song R, editors. Design and experimental research of an underwater vibration suction module inspired by octopus suckers. *ROBIO, 2017 IEEE International Conference on*. New York City, US: IEEE, 2017.
157. Kier WM, Smith AM. The structure and adhesive mechanism of octopus suckers. *ICB*. 2002;42:1146–53.
158. Hou J, Wright E, Bonser RH, Jeronimidis G. Development of biomimetic squid-inspired suckers. *J Bionic Eng*. 2012; 9:484–93.
159. Varenberg M, Gorb SN. Hexagonal surface micropattern for dry and wet friction. *Adv Mater*. 2009;21:483–6.
160. Wang S, Luo H, Linghu C, Song J. Elastic energy storage enabled magnetically actuated, octopus-inspired smart adhesive. *Adv Funct Mater*. 2021;31:2009217. https://doi.org/10.1002/adfm.202009217.
161. Dayan CB, Chun S, Krishna-Subbaiah N, Drotlef DM, Akolpoglu MB, Sitti M. 3D printing of elastomeric bioinspired complex adhesive microstructures. *Adv Mater*. 2021;33: 2103826. https://doi.org/10.1002/adma.202103826.
162. Baik S, Kim DW, Park Y, Lee T-J, Ho Bhang S, Pang C. A wet-tolerant adhesive patch inspired by protuberances in suction cups of octopi. *Nature*. 2017;546:396–400.
163. Chang W-Y, Wu Y, Chung Y-C. Facile fabrication of ordered nanostructures from protruding nanoballs to recessional nanosuckers via solvent treatment on covered nanosphere assembled monolayers. *Nano Lett*. 2014;14:1546–50.
164. Chen Y-C, Yang H. Octopus-inspired assembly of nanosucker arrays for dry/wet adhesion. *ACS Nano*. 2017;11:5332–8.
165. Kim DW, Baik S, Min H, Chun S, Lee HJ, Kim KH, *et al.* Highly permeable skin patch with conductive hierarchical architectures inspired by amphibians and octopi for omnidirectionally enhanced wet adhesion. *Adv Funct Mater*. 2019;29:1807614. https://doi.org/10.1002/adfm.201807614.
166. Liu Z, Wang X, Qi D, Xu C, Yu J, Liu Y, *et al.* High-adhesion stretchable electrodes based on Nanopile interlocking. *Adv Mater*. 2017;29:1603382. https://doi.org/10.1002/adma.201603382.
167. Chipara AC, Brunetto G, Özden Ş, Haspel H, Kumbhakar P, Kukovecz A, *et al.* Nature inspired solid-liquid phase amphibious adhesive. *Soft Matter*. 2020;16:5854–60.
168. Liimatainen V, Drotlef DM, Son D, Sitti M. Liquid-superrepellent bioinspired fibrillar adhesives. *Adv Mater*. 2020;32:2000497. https://doi.org/10.1002/adma.202000497.
169. Drotlef DM, Amjadi M, Yunusa M, Sitti M. Bioinspired composite microfibers for skin adhesion and signal amplification of wearable sensors. *Adv Mater*. 2017;29:1701353. https://doi.org/10.1002/adma.201701353.
170. Liang C, Ye Z, Xue B, Zeng L, Wu W, Zhong C, *et al.* Self-assembled nanofibers for strong underwater adhesion: the trick of barnacles. *ACS Appl Mater Interfaces*. 2018;10: 25017–25.
171. Mertens SF, Hemmi A, Muff S, Gröning O, De Feyter S, Osterwalder J, *et al.* Switching stiction and adhesion of a liquid on a solid. *Nature*. 2016;534:676–9.
172. Kizilkan E, Gorb SN. Combined effect of the microstructure and underlying surface curvature on the performance of biomimetic adhesives. *Adv Mater*. 2018;30:1704696. https://doi.org/10.1002/adma.201704696.
173. Barreau V, Hensel R, Guimard NK, Ghatak A, McMeeking RM, Arzt E. Fibrillar elastomeric micropatterns create tunable adhesion even to rough surfaces. *Adv Funct Mater*. 2016;26:4687–94.

174. Maier GP, Rapp MV, Waite JH, Israelachvili JN, Butler A. Adaptive synergy between catechol and lysine promotes wet adhesion by surface salt displacement. *Science*. 2015;349:628–32.
175. Xu X, Xia X, Zhang K, Rai A, Li Z, Zhao P, *et al.* Bioadhesive hydrogels demonstrating pH-independent and ultrafast gelation promote gastric ulcer healing in pigs. *Sci Transl Med*. 2020;12:aba8014. http://doi.10.1126/scitranslmed.aba8014.
176. Qi X, Yao X, Deng S, Zhou T, Fu Q. Water-induced shape memory effect of graphene oxide reinforced polyvinyl alcohol nanocomposites. *J Mater Chem A*. 2014;2:2240–9.
177. Xie T. Tunable polymer multi-shape memory effect. *Nature*. 2010;464:267–70.
178. Yang SY, O'Cearbhaill ED, Sisk GC, Park KM, Cho WK, Villiger M, *et al.* A bio-inspired swellable microneedle adhesive for mechanical interlocking with tissue. *Nat Commun*. 2013;4:1–10.
179. An R, Zhang X, Han L, Wang X, Zhang Y, Shi L, *et al.* Healing, flexible, high thermal sensitive dual-network ionic conductive hydrogels for 3D linear temperature sensor. *Mater Sci Eng C*. 2020;107:110310. https://doi.org/10.1016/j.msec.2019.110310.
180. Zeng Y, Li T, Yao Y, Li T, Hu L, Marconnet A. Thermally conductive reduced graphene oxide thin films for extreme temperature sensors. *Adv Funct Mater*. 2019;29:1901388. https://doi.org/10.1002/adfm.201901388.
181. Yao MS, Lv XJ, Fu ZH, Li WH, Deng WH, Wu GD, *et al.* Layer-by-layer assembled conductive metal–organic framework Nanofilms for room-temperature Chemiresistive sensing. *Angew Chem*. 2017;129:16737–41.
182. Montgomery M, Ahadian S, Huyer LD, Rito ML, Civitarese RA, Vanderlaan RD, *et al.* Flexible shape-memory scaffold for minimally invasive delivery of functional tissues. *Nat Mater*. 2017;16:1038–46.
183. North MA, Del Grosso CA, Wilker JJ. High strength underwater bonding with polymer mimics of mussel adhesive proteins. *ACS Appl Mater Interfaces*. 2017;9:7866–72.
184. Cui C, Wu T, Chen X, Liu Y, Li Y, Xu Z, *et al.* A Janus hydrogel wet adhesive for internal tissue repair and anti-postoperative adhesion. *Adv Funct Mater*. 2020;30:2005689.
185. Wang Y, Shang L, Chen G, Sun L, Zhang X, Zhao Y. Bioinspired structural color patch with anisotropic surface adhesion. *Sci Adv*. 2020;6:eaax8258. https://doi.10.1126/sciadv.aax8258.
186. Boutry CM, Beker L, Kaizawa Y, Vassos C, Tran H, Hinckley AC, *et al.* Biodegradable and flexible arterial-pulse sensor for the wireless monitoring of blood flow. *Nat Biomed Eng*. 2019;3:47–57.
187. Darabi MA, Khosrozadeh A, Wang Q, Xing M. Gum sensor: a stretchable, wearable, and foldable sensor based on carbon nanotube/chewing gum membrane. *ACS Appl Mater Interfaces*. 2015;7:26195–205.
188. Chang Q, Darabi MA, Liu Y, He Y, Zhong W, Mequanin K, *et al.* Hydrogels from natural egg white with extraordinary stretchability, direct-writing 3D printability and self-healing for fabrication of electronic sensors and actuators. *J Mater Chem A*. 2019;7:24626–40.
189. Chang Q, He Y, Liu Y, Zhong W, Wang Q, Lu F, *et al.* Protein gel phase transition: toward superiorly transparent and hysteresis-free wearable electronics. *Adv Funct Mater*. 2020;30:1910080. https://doi.org/10.1002/adfm.201910080.
190. Chun S, Son W, Kim DW, Lee J, Min H, Jung H, *et al.* Water-resistant and skin-adhesive wearable electronics using graphene fabric sensor with octopus-inspired microsuckers. *ACS Appl Mater Interfaces*. 2019;11:16951–7.